fractal and fractional

MDPI

Article

Exploring SEIR Influenza Epidemic Model via Fuzzy ABC Fractional Derivatives with Crowley–Martin Incidence Rate

F. Gassem [1], Ashraf A. Qurtam [2], Mohammed Almalahi [3,4], Mohammed Rabih [5,*], Khaled Aldwoah [6], Abdelaziz El-Sayed [7,*] and E. I. Hassan [8]

1 Department of Mathematics, College of Science, University of Ha'il, Ha'il 55473, Saudi Arabia
2 Biology Department, College of Science, Imam Mohammad Ibn Saud Islamic University (IMSIU), Riyadh 11432, Saudi Arabia
3 Department of Mathematics, College of Computer and Information Technology, Al-Razi University, Sana'a 12544, Yemen; dralmalahi@gmail.com
4 Jadara University Research Center, Jadara University, Irbid 21110, Jordan
5 Department of Mathematics, College of Science, Qassim University, Buraydah 51452, Saudi Arabia
6 Department of Mathematics, Faculty of Science, Islamic University of Madinah, Madinah 42351, Saudi Arabia; aldwoah@iu.edu.sa
7 Biology Department, Faculty of Science, Islamic University of Madinah, Madinah 42351, Saudi Arabia
8 Department of Mathematics and Statistics, Imam Mohammad Ibn Saud Islamic University (IMSIU), Riyadh 11432, Saudi Arabia
* Correspondence: m.fadlallah@qu.edu.sa (M.R.); aaelsayed@iu.edu.sa (A.E.-S.)

Abstract: Despite initial changes in respiratory illness epidemiology due to SARS-CoV-2, influenza activity has returned to pre-pandemic levels, highlighting its ongoing challenges. This paper investigates an influenza epidemic model using a Susceptible-Exposed-Infected-Recovered (SEIR) framework, extended with fuzzy Atangana–Baleanu–Caputo (ABC) fractional derivatives to incorporate uncertainty (via fuzzy numbers for state variables) and memory effects (via the ABC fractional derivative for non-local dynamics). We establish the theoretical foundation by defining the fuzzy ABC derivatives and integrals based on the generalized Hukuhara difference. The existence and uniqueness of the solutions for the fuzzy fractional SEIR model are rigorously proven using fixed-point theorems. Furthermore, we analyze the system's disease-free and endemic equilibrium points under the fractional framework. A numerical scheme based on the fractional Adams–Bashforth method is used to approximate the fuzzy solutions, providing interval-valued results for different uncertainty levels. The study demonstrates the utility of fuzzy fractional calculus in providing a more flexible and potentially realistic approach to modeling epidemic dynamics under uncertainty.

Keywords: influenza model; fuzzy ABC fractional operator; stability; simulation

Academic Editor: Zubair Ahmad

Received: 19 May 2025
Revised: 9 June 2025
Accepted: 16 June 2025
Published: 23 June 2025

Citation: Gassem, F.; Qurtam, A.A.; Almalahi, M.; Rabih, M.; Aldwoah, K.; El-Sayed, A.; Hassan, E.I. Exploring SEIR Influenza Epidemic Model via Fuzzy ABC Fractional Derivatives with Crowley–Martin Incidence Rate. *Fractal Fract.* **2025**, *9*, 402. https://doi.org/10.3390/fractalfract9070402

1. Introduction

Influenza, a highly contagious respiratory disease caused by influenza viruses, imposes significant annual health and economic burdens worldwide. It leads to millions of severe illnesses and deaths, particularly among vulnerable populations, such as the elderly and children, with the associated healthcare costs amounting to billions of dollars. Flu severity was mild in 2023–2024, with activity recovering to pre-pandemic levels [1]. The CDC predicted 40 million Americans would catch influenza, with 18 million seeking medical care, 470,000 hospitalized, and 28,000 deaths. Patients aged 65 and older accounted for 68% of the fatalities and 50% of the hospitalizations [2]. Unfortunately, the pandemic indirectly affected influenza immunization rates [3,4]. Primarily caused by influenza A

and B viruses in humans, the disease spreads readily via airborne droplets released during coughing, sneezing, or talking. Symptoms, often appearing suddenly, include fever, cough, sore throat, myalgia, headaches, and fatigue; vomiting and diarrhea may also occur, especially in children. While most individuals recover within one to two weeks without medical intervention, influenza can precipitate serious complications like pneumonia, bronchitis, and the exacerbation of chronic health conditions, especially in young children, older adults, pregnant women, and those with underlying health issues. Annual vaccination remains the most effective strategy for preventing influenza and its severe outcomes. Given its substantial global health impact, understanding the transmission dynamics of influenza is of paramount importance [5–7].

Mathematical modeling is a crucial tool for elucidating the transmission dynamics of infectious diseases and informing public health interventions [8–10]. The Susceptible-Exposed-Infected-Recovered (SEIR) model, a fundamental compartmental framework, is widely employed to describe the spread of diseases like influenza, where individuals undergo an exposed (latent) period before becoming infectious [11]. Classical SEIR models typically utilize integer-order ordinary differential equations, assuming that the rate of change depends solely on the current state and that parameters are precise [12–14]. However, real-world epidemiological systems often exhibit complexities not fully captured by these classical models. For instance, biological processes such as immune response duration, coupled with epidemiological factors like reporting delays and persistent environmental factors, can introduce memory effects, implying that the future state of the system depends not only on its present state but also on its past states. Fractional calculus [15–17], which extends differentiation and integration to arbitrary non-integer orders, provides powerful tools to incorporate such memory and hereditary properties into dynamical systems [18–20]. Notably, the Atangana–Baleanu–Caputo (ABC) derivative, characterized by its non-local and non-singular Mittag–Leffler kernel, has gained traction for its efficacy in modeling diverse real-world phenomena due to its ability to capture a wider range of memory effects [21–23]. Furthermore, inherent uncertainty and vagueness often characterize epidemiological data and parameters. Population counts, diagnostic accuracy, individual susceptibility, and infectiousness can be imprecise or challenging to measure accurately.

Fuzzy set theory, pioneered by Zadeh [24], offers a robust mathematical framework for managing such uncertainties by representing variables as fuzzy numbers rather than crisp values. The primary advantage of this approach in epidemiological modeling is its ability to capture the inherent vagueness and imprecision in real-world data. For instance, population counts are estimates, diagnostic tests have sensitivity and specificity limitations, and an individual's infectiousness is not a fixed constant. By using fuzzy numbers, we can represent a parameter like the transmission rate not as a single crisp value, but as a range of possibilities (e.g., 'around 0.9', represented by a fuzzy interval), which is often more realistic. Fuzzy data in practice can be derived from statistical confidence intervals of empirical data, from ranges provided in public health reports, or through expert elicitation. While the direct estimation of fuzzy parameters from raw data is a complex field in its own right, a common and practical approach, which we adopt in our numerical simulations, is to define fuzzy numbers based on the uncertainty ranges around established crisp values found in the literature. This allows us to demonstrate the model's capacity to handle and propagate uncertainty through the system's dynamics, yielding solutions as fuzzy bands that represent a range of potential epidemic trajectories. Previous studies have explored epidemic models using fuzzy fractional Caputo derivatives for childhood diseases [25], fuzzified models for dengue transmission [26], and fuzzy fractional SIS models for MERS-CoV [27].

While these approaches demonstrate the value of incorporating fractional dynamics and fuzzy logic, a comprehensive SEIR model for influenza that specifically leverages the fuzzy Atangana–Baleanu–Caputo (ABC) fractional derivative to simultaneously and effectively address both complex memory effects and inherent epidemiological uncertainties has not been fully developed and analyzed. The ABC derivative, with its non-singular kernel, is particularly well-suited for describing memory phenomena in biological systems compared with some other fractional operators [28–30].

Therefore, to address this gap, this paper introduces and analyzes an SEIR model for influenza transmission formulated using fuzzy ABC fractional derivatives. We extend the classical SEIR model by representing the population compartments (SEIR) as fuzzy-valued functions and employing fuzzy ABC fractional derivatives of order η. This approach enables the modeling of dynamics where the system's history influences its evolution (via the fractional derivative) and the state variables inherently incorporate imprecision (via fuzzy numbers). This work first establishes the requisite mathematical background before formulating the fuzzy ABC fractional SEIR model. A key contribution is the proof of existence and uniqueness of solutions, followed by an investigation of the disease-free and endemic equilibrium points. Subsequently, to demonstrate the model's practical behavior and the impact of uncertainty and memory, we develop a numerical scheme based on the fractional Adams–Bashforth technique. This allows us to generate and interpret interval-valued solutions under different assumptions, providing a tangible illustration of how this framework can offer a more nuanced understanding of epidemic dynamics.

While building on established principles, the primary contribution of this paper is the novel synthesis and comparative analysis of a fuzzy Atangana–Baleanu–Caputo (ABC) framework with a Crowley–Martin incidence rate for influenza modeling. The innovation lies not in creating new operators, but in demonstrating the unique and complex dynamics that emerge from this specific combination. A core element of our investigation is the rigorous analysis of how the choice of generalized Hukuhara (gH) differentiability (i)-gH versus (ii)-gH profoundly alters the predicted epidemic trajectories. As our results will show, this choice can mean the difference between predicting a classic epidemic wave and predicting a monotonic disease fade-out, a critical distinction for public health interpretation. By systematically exploring these dynamics, this work provides a deeper understanding of the interplay between memory effects, behavioral saturation, and uncertainty in epidemic modeling.

2. Basic Concepts and Supplementary Results

Here, we present the basic definitions of the ABC fractional operator through a fuzzy concept and outline fundamental theories. Moreover, we highlight key results that will be used throughout this paper.

Definition 1 ([31]). *A fuzzy number u is a map $u : \mathbb{R} \to \mathcal{J}$ such that u satisfies the following properties*

- *u is upper semi-continuous.*
- *u is fuzzy convex, i.e., $u(\lambda x + (1-\lambda)y) \geq \min\{u(x), u(y)\}, \forall\, x, y \in \mathbb{R}, \lambda \in [0,1]$.*
- *u is normal, i.e, $\exists x_0 \in \mathbb{R}; u(x_0) = 1$.*
- *The closure of $supp(u) = \{x \in \mathbb{R} : u(x) > 0\}$ is compact.*

Definition 2 ([31]). *The parametric interval form of fuzzy number u is given by*

$$[u]_\beta = [\underline{u}(\beta), \overline{u}(\beta)], \beta \in [0,1],$$

where $\underline{u}(\beta)$ and $\overline{u}(\beta)$ are continuous and nondecreasing functions on the left and right with respect to β such that $\forall \beta \in \mathcal{J}$, we have $\overline{u}(\beta) \geq \underline{u}(\beta)$.

Definition 3 ([31]). *The arithmetic operations (addition and scalar multiplication) of arbitrary fuzzy numbers $[u]_\beta$ and $[v]_\beta$ are given as*

$$\begin{aligned}(u \oplus v)[\beta] &= [\underline{u}(\beta) + \underline{v}(\beta), \overline{u}(\beta) + \overline{v}(\beta)],\\ (\lambda \odot u)[\beta] &= \begin{cases} [\lambda \underline{u}(\beta), \lambda \overline{u}(\beta)], \lambda \geq 0,\\ [\lambda \overline{u}(\beta), \lambda \underline{u}(\beta)], \lambda < 0,\end{cases}\end{aligned}$$

where $\beta \in \mathcal{J}$.

Let $[\rho(\iota)]_\beta \in C^F(\mathcal{J}, \mathbb{R}) \cap L^F(\mathcal{J}, \mathbb{R})$ be a fuzzy-valued function. Then, the parametric interval form of $\rho(\iota, \beta)$ is

$$[\rho(\iota)]_\beta = \left[\underline{\rho}(\iota, \beta), \overline{\rho}(\iota, \beta)\right], \beta \in [0, 1].$$

Definition 4 ([32]). *Let $\mathbb{R}_F$ be the set of all fuzzy numbers on real numbers and $(\mathbb{R}_F, d)$ a complete metric space. The Hausdorff distance is defined as the following:*

$$d : \mathbb{R}_F \times \mathbb{R}_F \to \mathbb{R}_+ \cup \{0\},$$

$$d(x, y) = \sup_{\beta \in [0,1]} \max\{|\underline{u}(\beta) - \underline{v}(\beta)|, |\overline{x}(\beta) - \overline{y}(\beta)|\}.$$

Then, the following properties are well known:

(1) $d(x \oplus w, y \oplus w) = d(x, y)$, for all $x, y, w \in \mathbb{R}_F$.
(2) $d(x \oplus w, 0) = d(x, 0) + d(y, 0)$, for all $x, y, w \in \mathbb{R}_F$.
(3) $d(x \oplus y, x \oplus w) = d(y, w)$, for all $x, y, w \in \mathbb{R}_F$.
(4) $d(x \oplus y, z \oplus w) \leq d(x, z) + d(y, w)$, for all $x, y, z, w \in \mathbb{R}_F$
(5) $d(x \ominus y, z \ominus w) \leq d(x, z) + d(y, w)$, for all $x, y, z, w \in \mathbb{R}_F, x \ominus y$ and $z \ominus w$ exist.
(6) $d(\lambda \odot x, \lambda \odot y) = |\lambda| d(x, y)$, for all $x, y \in \mathbb{R}_F, \lambda \in \mathbb{R}$.

Definition 5 ([33]). *Let $\mathbb{R}^F$ be the set of all fuzzy numbers and $u, v \in \mathbb{R}^F$. If there exists a fuzzy number $w \in \mathbb{R}^F$ such that $u = v + w$, then w is called the Hukuhara difference of u and v and it is denoted by $u \ominus v$.*

Definition 6. *The generalized Hukhara difference of two fuzzy numbers is defined as follows:*

$$u \ominus_{gH} v = w \iff \begin{cases} (i)\ \ u = v \oplus w,\\ (ii)\ v = u \oplus (-1)w.\end{cases}$$

The first case is equivalent to the Hukuhara difference, denoted by $u \ominus v$. If $[u]_\beta = [\underline{u}(\beta), \overline{u}(\beta)]$ and $[v]_\beta = [\underline{v}(\beta), \overline{v}(\beta)]$, there is

$$u \ominus_{gH} v = [\min\{\underline{u}(\beta) - \underline{v}(\beta), \overline{u}(\beta) - \overline{v}(\beta)\}, \max\{\underline{u}(\beta) - \underline{v}(\beta), \overline{u}(\beta) - \overline{v}(\beta)\}],$$

and the conditions for the existence of $u, v \in \mathbb{R}^F$ are as follows:

Case 1: $[w]_\beta = [\underline{w}(\beta), \overline{w}(\beta)] = [\underline{u}(\beta) - \underline{v}(\beta), \overline{u}(\beta) - \overline{v}(\beta)]$ with $\underline{w}(\beta)$ increasing; $\overline{w}(\beta)$ decreasing, $\underline{w}(\beta) \leq \overline{w}(\beta)$.

Case 2: $[w]_\beta = [\underline{w}(\beta), \overline{w}(\beta)] = [\overline{u}(\beta) - \overline{v}(\beta), \underline{u}(\beta) - \underline{v}(\beta)]$ with $\underline{w}(\beta)$ increasing; $\overline{w}(\beta)$ decreasing, $\underline{w}(\beta) \leq \overline{w}(\beta)$.

Definition 7 ([33]). *The generalized Hukuhara derivative of function $\rho(\iota)$ can be defined as*

$$ {}_{gH}\rho'(\iota) = \lim_{h\to 0^+} \frac{\rho(\iota+h) \ominus_{gH} \rho(\iota)}{h} = \lim_{h\to 0^+} \frac{\rho(\iota) \ominus_{gH} \rho(\iota+h)}{h}, \tag{1} $$

where

$$ {}_{gH}\rho'(\iota) \in C^F(I) \cap L^F(I), $$

and

$$ \rho(\iota+h) \ominus_{gH} \rho(\iota) = g(\iota) \Longleftrightarrow \begin{cases} i)\ \rho(\iota+h) = \rho(\iota) \oplus g(\iota), \\ ii)\ \rho(\iota) = \rho(\iota+h) \oplus (-1)g(\iota). \end{cases} \tag{2} $$

The first case reduced to the Hukuhara difference of $\rho(\iota+h) \ominus \rho(\iota)$. By applying a β-cut to both sides of (1), with the definition of the gH-difference (2), we obtain

- *Case (1) (i-Differentiability)*

$$ {}_{(i)-gH}\left[\rho'(\iota)\right]_\beta = \left[\underline{\rho}'(\iota,\beta), \overline{\rho}'(\iota,\beta)\right]. $$

- *Case (2) (ii-Differentiability)*

$$ {}_{(ii)-gH}\left[\rho'(\iota)\right]_\beta = \left[\overline{\rho}'(\iota,\beta), \underline{\rho}'(\iota,\beta)\right]. $$

The choice between these two cases of generalized Hukuhara differentiability is not arbitrary and has significant implications for the model's interpretation.

Case (1) (*i*-Differentiability): This case is analogous to the standard concept of a derivative. If a function is (i)-differentiable, the uncertainty (i.e., the width of the fuzzy interval) tends to be a non-decreasing function of time. This is appropriate for systems where initial uncertainties are expected to propagate and potentially grow over time.

Case (2) (*ii*-Differentiability): In this case, the derivative exists in a different sense, where the width of the fuzzy interval may decrease. This allows for the modeling of systems where uncertainty might reduce over time, for instance, as a system converges towards a stable, crisp equilibrium point.

The choice depends on the expected behavior of the system's uncertainty. In our study, we explore both scenarios to provide a comprehensive analysis. Case 1 (Figures 1–7) assumes all the state variables are (i)-differentiable, representing an unfolding epidemic with propagating uncertainty. Case 2 (Figures 8–11) assumes all are (ii)-differentiable, exploring a scenario more akin to disease fade-out or stabilization. This is made explicit in the header of each simulation section.

Definition 8 ([34]). *The Atangana–Baleanu derivative in the Caputo sense of a differentiable function $\rho(\iota)$ of order $\eta \in (0,1]$ is defined as*

$$ {}^{ABC}D_0^\eta \rho(\iota) = \frac{\Delta(\eta)}{1-\eta} \int_0^\iota E_\eta\left(\frac{-\eta}{\eta-1}(\iota-s)^\eta\right)\rho'(s)ds, $$

where $\Delta(\eta) = 1-\eta+\frac{\eta}{\Gamma(\eta)}$ and E_η is the ML function defined by $E_\eta(\iota) = \sum_{i=0}^{\infty} \frac{\iota^i}{\Gamma(i\eta+1)}$, $\Re(\eta) > 0$, $\iota \in \mathbb{C}$.

Definition 9 ([33]). *The ABC fractional derivative on fuzzy valued functions is given in two cases as follows*

$$ \left[{}_0^{ABC}D_\iota^{i,\eta}\rho(\iota)\right]_\beta = \left[{}_0^{ABC}D_\iota^{i,\eta}\underline{\rho}(\iota,\beta), {}_0^{ABC}D_\iota^{i,\eta}\overline{\rho}(\iota,\beta)\right],\ \textit{Case (1)}, $$

and

$$ \left[{}_0^{ABC}D_\iota^{ii,\eta}\rho(\iota)\right]_\beta = \left[{}_0^{ABC}D_\iota^{ii,\eta}\overline{\rho}(\iota,\beta), {}_0^{ABC}D_\iota^{i,\eta}\underline{\rho}(\iota,\beta)\right],\ \textit{Case (2)}, $$

where

$$\left[{}_0^{ABC}D_\iota^{i,\eta}\rho(\iota)\right]_\beta = \frac{\Delta(\eta)}{1-\eta}\int_0^\iota {}^{(i)-gH}\left[\rho'(\varsigma)\right]_\beta E_\eta\left(-\frac{\eta}{1-\eta}(\iota-\varsigma)^\eta\right)\Big|_{E_\eta\geq 0} d\iota + \frac{\Delta(\eta)}{1-\eta}\int_0^\iota {}^{(ii)-gH}\left[\rho'(\varsigma)\right]_\beta E_\eta\left(-\frac{\eta}{1-\eta}(\iota-\varsigma)^\eta\right)\Big|_{E_\eta<0} d\iota,$$

and

$$\left[{}_0^{ABC}D_\iota^{ii,\eta}\rho(\iota)\right]_\beta = \frac{\Delta(\eta)}{1-\eta}\int_0^\iota {}^{(ii)-gH}\left[\rho'(\varsigma)\right]_\beta E_\eta\left(-\frac{\eta}{1-\eta}(\iota-\varsigma)^\eta\right)\Big|_{E_\eta\geq 0} d\varsigma + \frac{\Delta(\eta)}{1-\eta}\int_0^\iota {}^{(i)-gH}\left[\rho'(\varsigma)\right]_\beta E_\eta\left(-\frac{\eta}{1-\eta}(\iota-\varsigma)^\eta\right)\Big|_{E_\eta<0} d\varsigma.$$

The end points of ABC fractional derivative are defined as,

$${}_0^{ABC}D_\iota^{*,\eta}\underline{\rho}(\iota,\beta) = \frac{\Delta(\eta)}{1-\eta}\int_0^\iota \underline{\rho}'(\varsigma,\beta)E_\eta\left(-\frac{\eta}{1-\eta}(\iota-\varsigma)^\eta\right)\Big|_{E_\eta\geq 0} d\varsigma + \frac{\Delta(\eta)}{1-\eta}\int_0^\iota \overline{\rho}'(\varsigma,\beta)E_\eta\left(-\frac{\eta}{1-\eta}(\iota-\varsigma)^\eta\right)\Big|_{E_\eta<0} d\varsigma,$$

and

$${}_0^{ABC}D_\iota^{*,\eta}\overline{\rho}(\iota,\beta) = \frac{\Delta(\eta)}{1-\eta}\int_0^\iota \overline{\rho}'(\varsigma,\beta)E_\eta\left(-\frac{\eta}{1-\eta}(\iota-\varsigma)^\eta\right)\Big|_{E_\eta\geq 0} d\varsigma + \frac{\Delta(\eta)}{1-\eta}\int_0^\iota \underline{\rho}'(\varsigma,\beta)E_\eta\left(-\frac{\eta}{1-\eta}(\iota-\varsigma)^\eta\right)\Big|_{E_\eta<0} d\varsigma,$$

and $* \in \{i, ii\}$.

The distinction based on the sign of the Mittag–Leffler kernel ($E_\eta \geq 0$ vs $E_\eta < 0$) relates to the nature of the system's memory. A non-negative kernel implies that past states always contribute positively (as a weighted average) to the current change, typical of accumulation or growth processes. A sign-changing kernel allows for more complex, non-monotonic memory effects, where past states might have an oscillating influence on the present, though this is less common in simple compartmental models.

Definition 10 ([34]). *The integral of the Atangana–Baleanu derivative in the Caputo sense of a differentiable function ρ of order $\eta \in (0,1]$ is defined as follows:*

$${}^{AB}I_0^\eta\rho(\iota) = \frac{1-\eta}{\Delta(\eta)}\rho(\iota) + \frac{\eta}{\Delta(\eta)}\frac{1}{\Gamma(\eta)}\int_0^\iota(\iota-s)^{\eta-1}\rho(s)ds.$$

Definition 11 ([33]). *The integral of the ABC fractional derivative for fuzzy-valued functions is given by*

$$\left[{}_0^{AB}I_\iota^\eta\rho(\iota)\right]_\beta = \left[{}_0^{ABC}I_\iota^\eta\underline{\rho}(\iota,\beta), {}_0^{ABC}I_\iota^\eta\overline{\rho}(\iota,\beta)\right],$$

where

$${}_0^{ABC}I_\iota^\eta\underline{\rho}(\iota,\beta) = \frac{1-\eta}{\Delta(\eta)}\underline{\rho}(\iota,\beta) + \frac{\eta}{\Delta(\eta)\Gamma(\eta)}\int_0^\iota(\iota-\varsigma)^{\eta-1}\underline{\rho}(\varsigma,\beta)d\varsigma,$$

and

$${}_0^{ABC}I_\iota^\eta\overline{\rho}(\iota,\beta) = \frac{1-\eta}{\Delta(\eta)}\overline{\rho}(\iota,\beta) + \frac{\eta}{\Delta(\eta)\Gamma(\eta)}\int_0^\iota(\iota-\varsigma)^{\eta-1}\overline{\rho}(\varsigma,\beta)d\varsigma.$$

Definition 12 ([33]). *Let* $\eta \in (0,1)$. *Then*

$$\left[{}_0^{AB}I_\iota^\eta\left({}_0^{AB}D_\iota^{i,\eta}\rho(\iota)\right)\right]_\beta = \left[{}_0^{AB}I_\iota^\eta\left({}_0^{ABC}D_\iota^{i,\eta}\underline{\rho}(\iota,\beta)\right), {}_0^{AB}I_\iota^\eta\left({}_0^{ABC}D_\iota^{i,\eta}\overline{\rho}(\iota,\beta)\right)\right], \text{ Case (1),}$$

and

$$\left[{}_0^{AB}I_\iota^\eta\left({}_0^{ABC}D_\iota^{ii,\eta}\rho(\iota)\right)\right]_\beta = \left[{}_0^{AB}I_\iota^\eta\left({}_0^{ABC}D_\iota^{ii,\eta}\overline{\rho}(\iota,\beta)\right), {}_0^{AB}I_\iota^\eta\left({}_0^{ABC}D_\iota^{ii,\eta}\underline{\rho}(\iota,\beta)\right)\right], \text{ Case (2),}$$

where

$${}_0^{AB}I_\iota^\eta\left({}_0^{ABC}D_\iota^{*,\eta}\underline{\rho}(\iota,\beta)\right) = \left(\underline{\rho}(\varsigma,\beta)-\underline{\rho}(0,\beta)\right)_{E_\eta\geq 0} + \left(\overline{\rho}(\varsigma,\beta)-\overline{\rho}(0,\beta)\right)_{E_\eta<0},$$

and

$${}_0^{AB}I_\iota^\eta\left({}_0^{ABC}D_\iota^{*,\eta}\overline{\rho}(\iota,\beta)\right) = \left(\overline{\rho}(\varsigma,\beta)-\overline{\rho}(0,\beta)\right)_{E_\eta\geq 0} + \left(\underline{\rho}(\varsigma,\beta)-\underline{\rho}(0,\beta)\right)_{E_\eta<0},$$

and $* \in \{i, ii\}$.

3. Mathematical Model

The authors in [12] studied the following Influenza Epidemic model SEIR. The SEIR framework is particularly suitable for influenza due to its well-documented latent period, where individuals are infected but not yet infectious (the 'Exposed' compartment)

$$\begin{aligned}
\frac{d}{d\iota}S(\iota) &= \Theta - \delta_1 S(\iota) - \frac{\delta_2 I(\iota)S(\iota)}{N},\\
\frac{d}{d\iota}E(\iota) &= \frac{\delta_2 I(\iota)S(\iota)}{N} - (\delta_1+\delta_3)E(\iota),\\
\frac{d}{d\iota}I(\iota) &= \delta_3 E(\iota) - (\delta_1+\delta_4)I(\iota),\\
\frac{d}{d\iota}R(\iota) &= \delta_4 I(\iota) - \delta_1 R(\iota),
\end{aligned}$$

where $\Theta = \delta_0 N$. In the above (SEIR) model, we divide the population into four distinct groups (compartments) based on their disease status, and the equations describe how individuals move between these compartments over time ι. The compartments are as follows:

$S(\iota)$: Susceptible: Individuals who are not yet infected but can become infected.

$E(\iota)$: Exposed: Individuals who have been infected but are not yet infectious to others (they are in the incubation period).

$I(\iota)$: Infectious: Individuals who are currently infected and can transmit the disease to susceptible individuals.

$R(\iota)$: Recovered: Individuals who have recovered from the infection and are assumed to be immune.

In this epidemiological framework, the population is categorized into four groups: Susceptible $S(\iota)$ (those who can contract the illness), Exposed $E(\iota)$ (those infected but not yet contagious), Infected $I(\iota)$ (those capable of transmitting the illness), and Recovered $R(\iota)$. The model accounts for demographic changes through a natural birth rate (adding to susceptibles) and a natural death rate (affecting all groups). Transmission of the virus from infected to susceptible individuals drives the epidemic. Key processes quantified include the rate of initial infection, the progression rate from exposed to infectious, and the rate of recovery, all while maintaining a constant overall population size. The model parameters and their estimates are defined in Table 1.

Table 1. The model parameters and their respective definitions.

Parameter	Definitions	Numerical Value	Ref
δ_0	Natural birth rate	0.00112	[10]
δ_1	Natural death rate	0.0013	[12]
δ_2	Transmission rate	0.97	[10]
δ_3	Incubation rate	0.78	[12]
δ_4	Recovery rate	0.62	[10]

4. Fractional Order Disease Model

To better represent the complex dynamics of disease evolution, this formulation extends the classical SEIR model, whose standard form often uses a bilinear incidence rate of the form $\frac{\beta I(\iota)S(\iota)}{N}$. Our proposed model replaces this with a Crowley–Martin type incidence rate [35], given by the term $\frac{\delta_2 I(\iota)S(\iota)}{(1+a_1 I(\iota))(1+a_2 S(\iota))}$. This non-linear incidence rate introduces two key behavioral or saturation effects. The term $(1 + a_2 S(\iota))$ in the denominator accounts for a saturation effect in the susceptible population, which can be interpreted as individuals reducing their number of contacts or taking more precautions as the number of available susceptible decreases or perceived risk changes. The term $(1 + a_1 I(\iota))$ represents an inhibition effect due to the infectious population, where susceptible individuals may further limit their contacts to avoid infection as the number of infected individuals increases. This makes the Crowley–Martin incidence rate more flexible and potentially more realistic than the simple bilinear or standard incidence rates, especially in populations where behavioral changes significantly impact transmission dynamics. The mathematical formulation of this model is as follows:

$$
\begin{aligned}
{}_0^{ABC}D_\iota^\eta S(\iota) &= \Theta - \delta_1 S(\iota) - \frac{\delta_2 I(\iota)S(\iota)}{(1 + a_1 I(\iota))(1 + a_2 S(\iota))}, && (3)\\
{}_0^{ABC}D_\iota^\eta E(\iota) &= \frac{\delta_2 I(\iota)S(\iota)}{(1 + a_1 I(\iota))(1 + a_2 S(\iota))} - (\delta_1 + \delta_3)E(\iota), && (4)\\
{}_0^{ABC}D_\iota^\eta I(\iota) &= \delta_3 E(\iota) - (\delta_1 + \delta_4)I(\iota), && (5)\\
{}_0^{ABC}D_\iota^\eta R(\iota) &= \delta_4 I(\iota) - \delta_1 R(\iota), && (6)
\end{aligned}
$$

where $S(\iota), E(\iota), I(\iota), R(\iota)$ represent the susceptible, exposed, infectious, and recovered populations at time ι, respectively. Θ is the recruitment rate into the susceptible population (e.g., births). δ_1 is the natural death rate, δ_2 is the transmission rate, δ_3 is the rate at which exposed individuals become infectious (incubation rate), and δ_4 is the recovery rate. The constants $a_1, a_2 > 0$ represent the strength of interference or saturation effects from infectious and susceptible individuals, respectively. The initial conditions are $S(0) \geq 0$, $E(0) \geq 0, I(0) \geq 0, R(0) \geq 0$.

The term "Fuzzy ABC derivatives" implies that either the parameters $(\Theta, \delta_i, a_i, \eta)$, the initial conditions, or the solutions themselves might be considered as fuzzy numbers. For the analytical discussion below, we primarily consider the deterministic skeleton of this model.

It should be noted that these parameter values are adopted from the cited literature to establish a consistent and verifiable baseline for demonstrating the proposed fuzzy fractional methodology. While fitting the model to specific, real-world influenza surveillance data would be a valuable and important extension, the primary focus of this study is on the theoretical development and numerical exploration of the model's framework. Such a data-driven application represents a key direction for future research.

4.1. Boundedness of Solutions

The total population is $N(\iota) = S(\iota) + E(\iota) + I(\iota) + R(\iota)$. Taking the fractional derivative of $N(\iota)$:

$$\begin{aligned}
{}_0^{ABC}D_\iota^\eta N(\iota) =& {}_0^{ABC}D_\iota^\eta S(\iota) + {}_0^{ABC}D_\iota^\eta E(\iota) + {}_0^{ABC}D_\iota^\eta I(\iota) + {}_0^{ABC}D_\iota^\eta R(\iota) \\
&= \Theta - \delta_1 S(\iota) - \frac{\delta_2 I(\iota) S(\iota)}{(1 + a_1 I(\iota))(1 + a_2 S(\iota))} \\
&+ \frac{\delta_2 I(\iota) S(\iota)}{(1 + a_1 I(\iota))(1 + a_2 S(\iota))} - (\delta_1 + \delta_3) E(\iota) \\
&+ (\delta_3 E(\iota) - (\delta_1 + \delta_4) I(\iota)) + (\delta_4 I(\iota) - \delta_1 R(\iota)) \\
&= \Theta - \delta_1 S(\iota) - \delta_1 E(\iota) - \delta_1 I(\iota) - \delta_1 R(\iota) \\
&= \Theta - \delta_1 N(\iota)
\end{aligned}$$

For the fractional differential equation ${}_0^{ABC}D_\iota^\eta N(\iota) = \Theta - \delta_1 N(\iota)$ with $N(0) \geq 0$, if $N(\iota) > \frac{\Theta}{\delta_1}$, then ${}_0^{ABC}D_\iota^\eta N(\iota) < 0$. This implies that $N(\iota)$ approaches $\frac{\Theta}{\delta_1}$ as $\iota \to \infty$. Thus, $N(\iota)$ is bounded by $\max(N(0), \frac{\Theta}{\delta_1})$. Since $S(\iota), E(\iota), I(\iota), R(\iota)$ are non-negative, they are also bounded. The feasible region for the model is as follows:

$$\Omega = \left\{ (S, E, I, R) \in \mathbb{R}_+^4 : S + E + I + R \leq \frac{\Theta}{\delta_1} \right\}.$$

All solutions starting in $\mathbb{R}_+^4$ eventually enter and remain in Ω.

4.2. Positivity of Solutions

It is important to note that the following analytical properties (positivity, boundedness, and the determination of equilibrium points) are investigated for the deterministic skeleton of the fuzzy model, where parameters and variables are treated as crisp values. This approach provides the essential mathematical foundation and stability thresholds (like $\mathcal{R}_0$) for the system. The significant difference introduced by the fuzzy ABC model lies not in these foundational proofs but in the numerical interpretation of the dynamics, where uncertainty is propagated over time. The impact of the fuzzy framework, which yields interval-valued solutions and provides a richer understanding of potential outcomes, is demonstrated in the numerical simulations section. For an epidemiological model to be biologically meaningful, all state variables must remain non-negative for all time $\iota \geq 0$, given non-negative initial conditions.

Theorem 1. *Let the initial conditions be $S(0) \geq 0, E(0) \geq 0, I(0) \geq 0, R(0) \geq 0$. Then the solutions $(S(\iota), E(\iota), I(\iota), R(\iota))$ of the model (3)–(6) are non-negative for all $\iota \geq 0$.*

Proof. Proving positivity for fractional-order systems rigorously often involves generalized mean value theorems or comparison principles for fractional derivatives. Heuristically

From (3), we have

$${}_0^{ABC}D_\iota^\eta S(\iota) \geq -\left(\delta_1 + \frac{\delta_2 I(\iota)}{(1 + a_1 I(\iota))(1 + a_2 S(\iota))} \right) S(\iota).$$

As all the solutions are bounded, therefore, we let $I(\iota)$ to be bounded by ψ. Then

$${}_0^{ABC}D_\iota^\eta S(\iota) \geq -mS(\iota), \tag{7}$$

where $m := \left(\delta_1 + \frac{\delta_2 \psi}{(1+a_1\psi)(1+a_2\psi)}\right)$ is a constant. Applying the Laplace transform on both sides of (7), we obtain

$$\frac{\Delta(\eta)s^{\eta-1}}{\eta+(1-\eta)s^{\eta}}\ell(S(\iota))(s) - \frac{\Delta(\eta)s^{\eta}}{\eta+(1-\eta)s^{\eta}}S(0) \geq -m\ell(S(\iota))(s),$$

and

$$\ell(S(\iota))(s) \geq \frac{\Delta(\eta)s^{\eta-1}S(0)}{\Delta(\eta)+m(1-\eta)}\frac{s^{\eta-1}}{s^{\eta}+\frac{m^{\eta}}{\Delta(\eta)+m(1-\eta)}}.$$

Now, by applying the inverse Laplace transform, we have

$$S(\iota) \geq \frac{\Delta(\eta)s^{\eta-1}S(0)}{\Delta(\eta)+m(1-\eta)}E_{\eta,1}\left(-\iota^{\eta}\frac{m^{\eta}}{\Delta(\eta)+m(1-\eta)}\right). \tag{8}$$

Thus, by positive value of the right-hand side of (8), we conclude that $S(\iota)$ remains positive for every $\iota \geq 0$. In the same manner, we deduce that $E(\iota) > 0$, $I(\iota) > 0$, and $R(\iota) > 0$, for every $\iota \geq 0$. As a result, the solutions in $\mathbb{R}^4_+$ will always be positive. □

Remark 1. *If the solutions are fuzzy numbers, positivity would mean that the support of these fuzzy numbers is contained within* $[0, \infty)$.

4.3. Equilibrium Points

Equilibrium points are found by setting the fractional derivatives to zero. In this part, we discuss the disease-free equilibrium (DFE) and endemic equilibrium (EE).

4.4. Disease-Free Equilibrium (DFE)

Let $I = 0$ in Equations (3)–(6). Then we have

$$0 = \Theta - \delta_1 S(\iota), \tag{9}$$
$$0 = -(\delta_1+\delta_3)E(\iota), \tag{10}$$
$$0 = \delta_3 E(\iota), \tag{11}$$
$$0 = -\delta_1 R(\iota). \tag{12}$$

From (11), we have

$$\delta_3 E = 0.$$

Since $\delta_3 > 0$,this implies that $E = 0$. By (12), we have

$$\delta_1 R = 0.$$

This implies that $R = 0$. By (9), we have

$$\Theta - \delta_1 S = 0.$$

This implies that $S = \frac{\Theta}{\delta_1}$. Thus, the DFE is

$$P = (\frac{\Theta}{\delta_1}, 0, 0, 0).$$

4.5. Endemic Equilibrium (EE)

To obtain the endemic equilibrium, we consider the new notation of S, E, I and R as $\widehat{S}, \widehat{E}, \widehat{I}$ and $\widehat{R}$. Then, we have

$$\begin{aligned}
{}_0^{ABC}D_\iota^\eta S(\iota) &= \Theta - \delta_1\widehat{S}(\iota) - \frac{\delta_2\widehat{I}(\iota)\widehat{S}(\iota)}{\left(1+a_1\widehat{I}(\iota)\right)\left(1+a_2\widehat{S}(\iota)\right)},\\
{}_0^{ABC}D_\iota^\eta E(\iota) &= \frac{\delta_2\widehat{I}(\iota)\widehat{S}(\iota)}{\left(1+a_1\widehat{I}(\iota)\right)\left(1+a_2\widehat{S}(\iota)\right)} - (\delta_1+\delta_3)\widehat{E}(\iota),\\
{}_0^{ABC}D_\iota^\eta I(\iota) &= \delta_3\widehat{E}(\iota) - (\delta_1+\delta_4)\widehat{I}(\iota),\\
{}_0^{ABC}D_\iota^\eta R(\iota) &= \delta_4\widehat{I}(\iota) - \delta_1\widehat{R}(\iota).
\end{aligned}$$

Let $\widehat{P} = (\widehat{S}, \widehat{E}, \widehat{I}, \widehat{R})$ be an endemic equilibrium where $\widehat{I} > 0$. Setting derivatives to zero:

$$0 = \Theta - \delta_1\widehat{S}(\iota) - \frac{\delta_2\widehat{I}(\iota)\widehat{S}(\iota)}{(1+a_1\widehat{I}(\iota))(1+a_2\widehat{S}(\iota))}, \tag{13}$$

$$0 = \frac{\delta_2\widehat{I}(\iota)\widehat{S}(\iota)}{(1+a_1\widehat{I}(\iota))(1+a_2\widehat{S}(\iota))} - (\delta_1+\delta_3)\widehat{E}(\iota), \tag{14}$$

$$0 = \delta_3\widehat{E}(\iota) - (\delta_1+\delta_4)\widehat{I}(\iota), \tag{15}$$

$$0 = \delta_4\widehat{I}(\iota) - \delta_1\widehat{R}(\iota), \tag{16}$$

From (15), we have

$$\widehat{E} = \frac{\delta_1+\delta_4}{\delta_3}\widehat{I}(\iota).$$

Let $k_1 = \delta_1 + \delta_3$ and $k_2 = \delta_1 + \delta_4$. So

$$\widehat{E} = \frac{k_2}{\delta_3}\widehat{I}(\iota).$$

From (16), we have

$$\widehat{R} = \frac{\delta_4}{\delta_1}\widehat{I}.$$

Substitute $\widehat{E}$ into (14) (assuming $\widehat{I} > 0$):

$$\frac{\delta_2\widehat{S}(\iota)}{(1+a_1\widehat{I}(\iota))(1+a_2\widehat{S}(\iota))} = k_1\frac{\widehat{E}(\iota)}{\widehat{I}(\iota)} = k_1\frac{k_2}{\delta_3}. \tag{17}$$

From (13), also using (14):

$$\Theta - \delta_1\widehat{S}(\iota) - k_1\widehat{E}(\iota) = 0 \implies \Theta - \delta_1\widehat{S}(\iota) - k_1\frac{k_2}{\delta_3}\widehat{I}(\iota) = 0.$$

So,

$$\widehat{I} = \frac{\delta_3(\Theta - \delta_1\widehat{S}(\iota))}{k_1k_2}. \tag{18}$$

Substituting (18) into (17), we obtain

$$\frac{\delta_2\widehat{S}(\iota)}{\left(1+a_1\frac{\delta_3(\Theta-\delta_1\widehat{S}(\iota))}{k_1k_2}\right)(1+a_2\widehat{S}(\iota))} = \frac{k_1k_2}{\delta_3}.$$

This equation can be rearranged into a polynomial in $\widehat{S}$. Specifically, it becomes a quadratic equation:

$$\delta_2\widehat{S}(\iota)\delta_3 = \frac{k_1k_2}{\delta_3}\Big(1+a_2\widehat{S}(\iota)\Big)\left(1+a_1\frac{\delta_3(\Theta-\delta_1\widehat{S}(\iota))}{k_1k_2}\right).$$

$$\delta_2\widehat{S}(\iota)\delta_3 = C_0(1+a_2\widehat{S}(\iota))\Big(1+C_1(\Theta-\delta_1\widehat{S}(\iota))\Big).$$

where $C_0 = \frac{k_1k_2}{\delta_3}$ and $C_1 = \frac{a_1\delta_3}{k_1k_2}$. Expanding this leads to the following:

$$A(\widehat{S}(\iota))^2 + B\widehat{S}(\iota) + C = 0.$$

where coefficients A, B, C depend on the model parameters. The existence and uniqueness of a positive $\widehat{S}(\iota) < \frac{\Theta}{\delta_1}$ (which implies $\widehat{I}(\iota) > 0$) typically depends on whether the basic reproduction number $\mathcal{R}_0 > 1$.

4.6. Basic Reproduction Number ($\mathcal{R}_0$)

The basic reproduction number $\mathcal{R}_0$ is calculated using the next-generation matrix method at the DFE $P = (\frac{\Theta}{\delta_1}, 0, 0, 0)$. The compartments involved in new infections are E and I. The linearized system for new infections ($\mathcal{F}$) and transitions ($\mathcal{V}$) for (E, I) is as follows:

$$\begin{pmatrix} {}^{ABC}_{0}D^{\eta}_{\iota}E(\iota) \\ {}^{ABC}_{0}D^{\eta}_{\iota}I(\iota) \end{pmatrix} = (F-V)\begin{pmatrix} E(\iota) \\ I(\iota) \end{pmatrix}$$

At DFE P, we have $S = \frac{\Theta}{\delta_1}$. The rate of new infections entering E is $\frac{\delta_2 IS}{(1+a_1I)(1+a_2S)}$. Linearizing this term with respect to I at $S = \frac{\Theta}{\delta_1}, I = 0$, we obtain

$$\frac{\partial}{\partial I}\left(\frac{\delta_2 IS}{(1+a_1I)(1+a_2S)}\right)\Bigg|_{I=0,S=\frac{\Theta}{\delta_1}} = \frac{\delta_2\frac{\Theta}{\delta_1}}{(1+0)(1+a_2\frac{\Theta}{\delta_1})} = \frac{\delta_2\frac{\Theta}{\delta_1}}{1+a_2\frac{\Theta}{\delta_1}}.$$

The matrices F (new infections) and V (transfers) are as follows:

$$F = \begin{pmatrix} 0 & \frac{\delta_2\frac{\Theta}{\delta_1}}{1+a_2\frac{\Theta}{\delta_1}} \\ 0 & 0 \end{pmatrix}, \quad V = \begin{pmatrix} \delta_1+\delta_3 & 0 \\ -\delta_3 & \delta_1+\delta_4 \end{pmatrix}$$

Then

$$V^{-1} = \frac{1}{(\delta_1+\delta_3)(\delta_1+\delta_4)}\begin{pmatrix} \delta_1+\delta_4 & 0 \\ \delta_3 & \delta_1+\delta_3 \end{pmatrix}.$$

The next-generation matrix is $K = FV^{-1}$:

$$K = \frac{1}{(\delta_1+\delta_3)(\delta_1+\delta_4)}\begin{pmatrix} 0 & \frac{\delta_2\frac{\Theta}{\delta_1}}{1+a_2\frac{\Theta}{\delta_1}} \\ 0 & 0 \end{pmatrix}\begin{pmatrix} \delta_1+\delta_4 & 0 \\ \delta_3 & \delta_1+\delta_3 \end{pmatrix}.$$

This implies

$$K = \frac{1}{(\delta_1+\delta_3)(\delta_1+\delta_4)}\begin{pmatrix} \frac{\delta_2\frac{\Theta}{\delta_1}\delta_3}{1+a_2\frac{\Theta}{\delta_1}} & \frac{\delta_2\frac{\Theta}{\delta_1}(\delta_1+\delta_3)}{1+a_2\frac{\Theta}{\delta_1}} \\ 0 & 0 \end{pmatrix}.$$

The basic reproduction number $\mathcal{R}_0$ is the spectral radius of K, $\rho(K)$. Then, we have

$$\mathcal{R}_0 = \frac{\delta_2 \frac{\Theta}{\delta_1} \delta_3}{(1 + a_2 \frac{\Theta}{\delta_1})(\delta_1 + \delta_3)(\delta_1 + \delta_4)} = \frac{\delta_2 \Theta \delta_3}{(\delta_1 + a_2 \Theta)(\delta_1 + \delta_3)(\delta_1 + \delta_4)}.$$

The Crowley–Martin term $\frac{1}{1+a_2 \frac{\Theta}{\delta_1}}$ reduces $\mathcal{R}_0$ compared with a standard incidence, reflecting the saturation effects at high susceptible densities. The $a_1 I$ term has no effect on $\mathcal{R}_0$ as it vanishes at $I = 0$.

4.7. Stability Analysis

The stability of equilibria for fractional-order systems depends on the arguments of the eigenvalues of the Jacobian matrix. An equilibrium is locally asymptotically stable if all eigenvalues λ_i of its Jacobian matrix satisfy|

$$\arg(\lambda_i)| > \eta \frac{\pi}{2}.$$

If $\eta = 1$, this reduces to $\mathrm{Re}(\lambda_i) < 0$.

4.8. Local Stability of DFE (P)

Let $\mathcal{I}(S, I) = \frac{\delta_2 IS}{(1+a_1 I)(1+a_2 S)}$. Then, $\frac{\partial \mathcal{I}}{\partial S}\Big|_{P=(\frac{\Theta}{\delta_1},0,0,0)} = 0$ (since $I = 0$), and $\frac{\partial \mathcal{I}}{\partial I}\Big|_{P=(\frac{\Theta}{\delta_1},0,0,0)} = \frac{\delta_2 \frac{\Theta}{\delta_1}}{1+a_2 \frac{\Theta}{\delta_1}}$ (as calculated for $\mathcal{R}_0$). The Jacobian matrix J for the model (3)–(6) evaluated at $P = (\frac{\Theta}{\delta_1}, 0, 0, 0)$ is given as follows:

$$J(P) = \begin{pmatrix} -\delta_1 & 0 & -\frac{\delta_2 \frac{\Theta}{\delta_1}}{1+a_2 \frac{\Theta}{\delta_1}} & 0 \\ 0 & -(\delta_1 + \delta_3) & \frac{\delta_2 \frac{\Theta}{\delta_1}}{1+a_2 \frac{\Theta}{\delta_1}} & 0 \\ 0 & \delta_3 & -(\delta_1 + \delta_4) & 0 \\ 0 & 0 & \delta_4 & -\delta_1 \end{pmatrix}$$

The eigenvalues are $-\delta_1$ (from the first row/column, associated with S), $-\delta_1$ (from the fourth row/column, associated with R), and the eigenvalues of the submatrix:

$$J_{EI} = \begin{pmatrix} -(\delta_1 + \delta_3) & \frac{\delta_2 \frac{\Theta}{\delta_1}}{1+a_2 \frac{\Theta}{\delta_1}} \\ \delta_3 & -(\delta_1 + \delta_4) \end{pmatrix}$$

We know that the characteristic equation for J_{EI} is

$$\lambda^2 - \mathrm{tr}(J_{EI})\lambda + \det(J_{EI}) = 0.$$

Thus, we have

$$\lambda^2 + ((\delta_1 + \delta_3) + (\delta_1 + \delta_4))\lambda + (\delta_1 + \delta_3)(\delta_1 + \delta_4) - \frac{\delta_2 \frac{\Theta}{\delta_1} \delta_3}{1 + a_2 \frac{\Theta}{\delta_1}} = 0.$$

Let $k_1 = (\delta_1 + \delta_3) > 0, k_2 = (\delta_1 + \delta_4) > 0$, then we have

$$\lambda^2 + (k_1 + k_2)\lambda + k_1 k_2 \left(1 - \frac{\delta_2 \frac{\Theta}{\delta_1} \delta_3}{(1 + a_2 \frac{\Theta}{\delta_1}) k_1 k_2}\right) = 0.$$

Thus,

$$\lambda^2 + (k_1 + k_2)\lambda + k_1 k_2 (1 - \mathcal{R}_0) = 0$$

If $\mathcal{R}_0 < 1$, then $1 - \mathcal{R}_0 > 0$. Since $k_1, k_2 > 0$, all the coefficients of the polynomial are positive. For integer-order systems ($\eta = 1$), this implies that the eigenvalues have negative real parts by the Routh–Hurwitz criterion. For fractional systems ($\eta \in (0, 1]$), if $\mathcal{R}_0 < 1$, the DFE is locally asymptotically stable. If $\mathcal{R}_0 > 1$, then $1 - \mathcal{R}_0 < 0$, leading to one positive real eigenvalue, making the DFE unstable.

4.9. Local Stability of Endemic Equilibrium ($\widehat{P}$)

If $\mathcal{R}_0 > 1$, an endemic equilibrium $\widehat{P}$ may exist. Its stability analysis involves calculating the Jacobian $J(\widehat{P})$ and examining its eigenvalues. This is algebraically intensive. Typically, if $\widehat{P}$ exists and is unique, it is locally asymptotically stable when $\mathcal{R}_0 > 1$. Proving this often requires specific conditions on parameters or using advanced techniques like Lyapunov functions adapted for fractional systems or geometric approaches.

4.10. Global Stability

Proving global stability for fractional-order nonlinear systems is a significant challenge. It usually involves constructing a suitable Lyapunov function and showing that its fractional derivative along the trajectories is negative definite. For DFE, global stability when $\mathcal{R}_0 < 1$ is often conjectured or proven under specific conditions. Global stability of EE when $\mathcal{R}_0 > 1$ is even more complex.

Remark 2. *When parameters or the fractional order η are fuzzy, stability becomes a fuzzy concept. One might analyze the stability of the system for a range of crisp parameter values within the support of the fuzzy numbers or use specific methods for fuzzy differential equations. The stability region in parameter space might itself be a fuzzy set. The ABC derivative's non-local nature (memory effect) introduced by the fractional order η significantly impacts the dynamics, and the value of η also influences the stability conditions and convergence rates.*

5. Fuzzy ABC Fractional Model

In this section, we transition from the deterministic model described in Equations (3)–(6) to its full fuzzy counterpart. The following model (19) is the direct fuzzy analogue, where the state variables and parameters are treated as fuzzy numbers to explicitly incorporate uncertainty. This is achieved by replacing standard arithmetic operations with their fuzzy equivalents, based on the principles of fuzzy calculus and the generalized Hukuhara difference. Here, we present the model in the fuzzy concept as follows:

$$\begin{cases} {}^{ABC}_{0}D_{\iota}^{*_1,\eta}\widetilde{S}(\iota) = \Theta \ominus_{gH} [\delta_1 \odot S(\iota)] \ominus_{gH} \left[\frac{\delta_2 \odot I(\iota) \odot S(\iota)}{I(\iota) \oplus S(\iota)}\right], \\ {}^{ABC}_{0}D_{\iota}^{*_2,\eta}\widetilde{E}(\iota) = \left[\frac{\delta_2 \odot I(\iota) \odot S(\iota)}{I(\iota) \oplus S(\iota)}\right] \ominus_{gH} [(\delta_1 \oplus \delta_3) \odot E(\iota)], \\ {}^{ABC}_{0}D_{\iota}^{*_3,\eta}\widetilde{I}(\iota) = [\delta_3 \odot E(\iota)] \ominus_{gH} [(\delta_1 \oplus \delta_4) \odot I(\iota)], \\ {}^{ABC}_{0}D_{\iota}^{*_4,\eta}\widetilde{R}(\iota) = [\delta_4 \odot I(\iota)] \ominus_{gH} [\delta_1 \odot R(\iota)]. \end{cases} \tag{19}$$

where $*_1, *_2, *_3, *_4 \in \{i, ii\}$, $\eta \in (0, 1)$, and $0 < \iota < T < \infty, T \in \mathbb{R}$. To obtain the fuzzy solution for (19), we assume

$$\begin{cases} F_1\left(\iota, \widetilde{S}, \widetilde{E}, \widetilde{I}, \widetilde{R}\right) = \Theta \ominus_{gH} \delta_1 \odot S(\iota) \ominus_{gH} \frac{\delta_2 \odot I(\iota) \odot S(\iota)}{I(\iota) \oplus S(\iota)}, \\ F_2\left(\iota, \widetilde{S}, \widetilde{E}, \widetilde{I}, \widetilde{R}\right) = \frac{\delta_2 \odot I(\iota) \odot S(\iota)}{I(\iota) \oplus S(\iota)} \ominus_{gH} (\delta_1 \oplus \delta_3) \odot E(\iota), \\ F_3\left(\iota, \widetilde{S}, \widetilde{E}, \widetilde{I}, \widetilde{R}\right) = \delta_3 \odot E(\iota) \ominus_{gH} (\delta_1 \oplus \delta_4) \odot I(\iota), \\ F_4\left(\iota, \widetilde{S}, \widetilde{E}, \widetilde{I}, \widetilde{R}\right) = \delta_4 \odot I(\iota) \ominus_{gH} \delta_1 \odot R(\iota). \end{cases} \tag{20}$$

Thus, we rewrite the model (19) as follows

$$\begin{cases} {}^{ABC}_{0}D_{\iota}^{*_1,\eta}\widetilde{S}(\iota) = F_1\Big(\iota,\widetilde{S},\widetilde{E},\widetilde{I},\widetilde{R}\Big), \\ {}^{ABC}_{0}D_{\iota}^{*_2,\eta}\widetilde{E}(\iota) = F_2\Big(\iota,\widetilde{S},\widetilde{E},\widetilde{I},\widetilde{R}\Big), \\ {}^{ABC}_{0}D_{\iota}^{*_3,\eta}\widetilde{I}(\iota) = F_3\Big(\iota,\widetilde{S},\widetilde{E},\widetilde{I},\widetilde{R}\Big), \\ {}^{ABC}_{0}D_{\iota}^{*_4,\eta}\widetilde{R}(\iota) = F_4\Big(\iota,\widetilde{S},\widetilde{E},\widetilde{I},\widetilde{R}\Big), \\ \widetilde{S}(0) = \widetilde{S}_0 > 0, \\ \widetilde{E}(0) = \widetilde{E}_0 > 0, \\ \widetilde{I}(0) = \widetilde{I}_0 > 0, \\ \widetilde{R}(0) = \widetilde{R}_0 > 0, \end{cases} \tag{21}$$

where $*_1, *_2, *_3, *_4 \in \{i, ii\}$, $\eta \in (0,1)$, and $0 < \iota < T < \infty, T \in \mathbb{R}$. When solving model, different cases can occur as in Table 2:

Table 2. Different cases of solutions.

Case	1	2	3	4	5	6	7	8	9	10	11	12	13	14	15	16
$*_1$	i	i	i	i	i	i	i	i	ii	ii	ii	ii	ii	ii	ii	ii
$*_2$	i	i	i	i	ii	ii	ii	ii	i	i	i	i	ii	ii	ii	ii
$*_3$	i	i	ii	ii	i	i	ii	ii	i	i	ii	ii	i	i	ii	ii
$*_4$	i	ii	i	ii	i	ii	i	ii	i	ii	i	ii	i	ii	i	ii

5.1. Existence of Unique Solution

Theorem 2. *Suppose that the functions $F_i\Big(\iota,\widetilde{S},\widetilde{E},\widetilde{I},\widetilde{R}\Big), i = 1,2,3,4$ in (21) are fuzzy-valued continuous functions defined in domain G, and satisfying the Lipschitz condition in G with respect to $\widetilde{S},\widetilde{E},\widetilde{I},\widetilde{R}$, and if $\exists M_k > 0, k = 1,2,3,4$, such that*

$$\begin{aligned} d\Big(F_1\Big(\iota,\widetilde{S}_1,\widetilde{E},\widetilde{I},\widetilde{R}\Big),F_1\Big(\iota,\widetilde{S}_2,\widetilde{E},\widetilde{I},\widetilde{R}\Big)\Big) &\leq M_1 d\Big(\widetilde{S}_1(\iota),\widetilde{S}_2(\iota)\Big), \\ d\Big(F_2\Big(\iota,\widetilde{S},\widetilde{E}_1,\widetilde{I},\widetilde{R}\Big),F_2\Big(\iota,\widetilde{S},\widetilde{E}_2,\widetilde{I},\widetilde{R}\Big)\Big) &\leq M_2 d\Big(\widetilde{E}_1(\iota),\widetilde{E}_2(\iota)\Big), \\ d\Big(F_3\Big(\iota,\widetilde{S},\widetilde{E},\widetilde{I}_1,\widetilde{R}\Big),F_3\Big(\iota,\widetilde{S},\widetilde{E},\widetilde{I}_2,\widetilde{R}\Big)\Big) &\leq M_3 d\Big(\widetilde{I}_1(\iota),\widetilde{I}_2(\iota)\Big), \\ d\Big(F_4\Big(\iota,\widetilde{S},\widetilde{E},\widetilde{I},\widetilde{R}_1\Big),F_4\Big(\iota,\widetilde{S},\widetilde{E},\widetilde{I},\widetilde{R}_2\Big)\Big) &\leq M_4 d\Big(\widetilde{R}_1(\iota),\widetilde{R}_2(\iota)\Big), \end{aligned}$$

$\forall \widetilde{S}_1,\widetilde{E}_1,\widetilde{I}_1,\widetilde{R}_1,\widetilde{S}_2,\widetilde{E}_2,\widetilde{I}_2,\widetilde{R}_2 \in G$. Then, the model (21) has a unique fuzzy number solutions $\widetilde{S}(\iota),\widetilde{E}(\iota),\widetilde{I}(\iota),\widetilde{R}(\iota)$, provided that

$$\left(\frac{1-\eta}{\Delta(\eta)} + \frac{\eta}{\Delta(\eta)\Gamma(\eta+1)}\right) \max_{k=1}^{4}\{M_k\} T^{\eta+1} < 1.$$

Proof. Define the operator $Z : C^F(\mathcal{J},\mathbb{R}) \cap L^F(\mathcal{J},\mathbb{R}) \to C^F(\mathcal{J},\mathbb{R}) \cap L^F(\mathcal{J},\mathbb{R})$ on the solutions with non-negative and negative kernels separately. We start by first case with $*_1, *_2, *_3, *_4 = i$, we define

$$\begin{cases} Z\Big(\widetilde{S}(\iota)\Big) = \widetilde{S}_0 \oplus \frac{1-\eta}{\Delta(\eta)} \odot F_1\Big(\iota,\widetilde{S},\widetilde{E},\widetilde{I},\widetilde{R}\Big) \oplus \frac{\eta}{\Delta(\eta)\Gamma(\eta)} \odot \int_0^{\iota}(\iota-\varsigma)^{\eta-1} \odot F_1\Big(\varsigma,\widetilde{S},\widetilde{E},\widetilde{I},\widetilde{R}\Big)d\varsigma, \\ Z\Big(\widetilde{E}(\iota)\Big) = \widetilde{E}_0 \oplus \frac{1-\eta}{\Delta(\eta)} \odot F_2\Big(\iota,\widetilde{S},\widetilde{E},\widetilde{I},\widetilde{R}\Big) \oplus \frac{\eta}{\Delta(\eta)\Gamma(\eta)} \odot \int_0^{\iota}(\iota-\varsigma)^{\eta-1} \odot F_2\Big(\varsigma,\widetilde{S},\widetilde{E},\widetilde{I},\widetilde{R}\Big)d\varsigma, \\ Z\Big(\widetilde{I}(\iota)\Big) = \widetilde{I}_0 \oplus \frac{1-\eta}{\Delta(\eta)} \odot F_3\Big(\iota,\widetilde{S},\widetilde{E},\widetilde{I},\widetilde{R}\Big) \oplus \frac{\eta}{\Delta(\eta)\Gamma(\eta)} \odot \int_0^{\iota}(\iota-\varsigma)^{\eta-1} \odot F_3\Big(\varsigma,\widetilde{S},\widetilde{E},\widetilde{I},\widetilde{R}\Big)d\varsigma, \\ Z\Big(\widetilde{R}(\iota)\Big) = \widetilde{R}_0 \oplus \frac{1-\eta}{\Delta(\eta)} \odot F_4\Big(\iota,\widetilde{S},\widetilde{E},\widetilde{I},\widetilde{R}\Big) \oplus \frac{\eta}{\Delta(\eta)\Gamma(\eta)} \odot \int_0^{\iota}(\iota-\varsigma)^{\eta-1} \odot F_4\Big(\varsigma,\widetilde{S},\widetilde{E},\widetilde{I},\widetilde{R}\Big)d\varsigma. \end{cases}$$

Let $\widetilde{S}_1, \widetilde{E}_1, \widetilde{I}_1, \widetilde{R}_1, \widetilde{S}_2, \widetilde{E}_2, \widetilde{I}_2, \widetilde{R}_2 \in G$. Then,

$$\begin{aligned} d\Big(Z\Big(\widetilde{S}_1(\iota)\Big), Z\Big(\widetilde{S}_2(\iota)\Big)\Big) &= d\Big(\frac{1-\eta}{\Delta(\eta)} \odot F_1\Big(\iota, \widetilde{S}_1, \widetilde{E}, \widetilde{I}, \widetilde{R}\Big) \oplus \frac{\eta}{\Delta(\eta)\Gamma(\eta)} \\ &\quad \odot \int_0^\iota (\iota-\varsigma)^{\eta-1} \odot F_1\Big(\varsigma, \widetilde{S}_1, \widetilde{E}, \widetilde{I}, \widetilde{R}\Big) d\varsigma, \\ &\quad \frac{1-\eta}{\Delta(\eta)} \odot F_1\Big(\iota, \widetilde{S}_2, \widetilde{E}, \widetilde{I}, \widetilde{R}\Big) \oplus \frac{\eta}{\Delta(\eta)\Gamma(\eta)} \\ &\quad \odot \int_0^\iota (\iota-\varsigma)^{\eta-1} \odot F_1\Big(\varsigma, \widetilde{S}_2, \widetilde{E}, \widetilde{I}, \widetilde{R}\Big) d\varsigma\Big). \end{aligned}$$

And based on the properties of the fuzzy metric from Definition 4 and the rules of fuzzy arithmetic, we have

$$\begin{aligned} d\Big(Z\Big(\widetilde{S}_1(\iota)\Big), Z\Big(\widetilde{S}_2(\iota)\Big)\Big) &\leq d\Big(\frac{1-\eta}{\Delta(\eta)} \odot F_1\Big(\iota, \widetilde{S}_1, \widetilde{E}, \widetilde{I}, \widetilde{R}\Big), \frac{1-\eta}{\Delta(\eta)} \odot F_1\Big(\iota, \widetilde{S}_2, \widetilde{E}, \widetilde{I}, \widetilde{R}\Big)\Big) \\ &\quad + d\Big(\frac{\eta}{\Delta(\eta)\Gamma(\eta)} \odot \int_0^\iota (\iota-\varsigma)^{\eta-1} \odot F_1\Big(\varsigma, \widetilde{S}_1, \widetilde{E}, \widetilde{I}, \widetilde{R}\Big) d\varsigma, \\ &\quad \frac{\eta}{\Delta(\eta)\Gamma(\eta)} \odot \int_0^\iota (\iota-\varsigma)^{\eta-1} \odot F_1\Big(\varsigma, \widetilde{S}_2, \widetilde{E}, \widetilde{I}, \widetilde{R}\Big) d\varsigma\Big) \\ &\leq \frac{1-\eta}{\Delta(\eta)} d\Big(F_1\Big(\iota, \widetilde{S}_1(\iota)\Big), F_1\Big(\iota, \widetilde{S}_2(\iota)\Big)\Big) + \frac{\eta}{\Delta(\eta)\Gamma(\eta)} \times \\ &\quad d\Big(\int_0^\iota (\iota-\varsigma)^{\eta-1} F_1\Big(\varsigma, \widetilde{S}_1(\varsigma)\Big) d\varsigma, \int_0^\iota (\iota-\varsigma)^{\eta-1} F_1\Big(\varsigma, \widetilde{S}_1(\varsigma)\Big) d\varsigma\Big) \\ &\leq \frac{1-\eta}{\Delta(\eta)} M_1 d\Big(\widetilde{S}_1(\iota), \widetilde{S}_2(\iota)\Big) + \frac{\eta}{\Delta(\eta)\Gamma(\eta)} \\ &\quad \int_0^\iota \Big|(\iota-\varsigma)^{\eta-1}\Big| d\Big(F_1\Big(\varsigma, \widetilde{S}_1(\varsigma)\Big), F_1\Big(\varsigma, \widetilde{S}_1(\varsigma)\Big)\Big) d\varsigma \\ &= \frac{1-\eta}{\Delta(\eta)} M_1 d\Big(\widetilde{S}_1(\iota), \widetilde{S}_2(\iota)\Big) + \frac{\eta}{\Delta(\eta)\Gamma(\eta)} M_1 d\Big(\widetilde{S}_1(\iota), \widetilde{S}_2(\iota)\Big) \\ &\quad \int_0^\iota \Big|(\iota-\varsigma)^{\eta-1}\Big| d\varsigma. \end{aligned}$$

$$d\Big(Z\Big(\widetilde{S}_1(\iota)\Big), Z\Big(\widetilde{S}_2(\iota)\Big)\Big) \leq \Big(\frac{1-\eta}{\Delta(\eta)} + \frac{\eta T^\eta}{\Delta(\eta)\Gamma(\eta+1)}\Big) M_1 d\Big(\widetilde{S}_1(\iota), \widetilde{S}_2(\iota)\Big).$$

In the same manner, we obtain

$$\begin{aligned} d\Big(Z\Big(\widetilde{E}_1(\iota)\Big), Z\Big(\widetilde{E}_2(\iota)\Big)\Big) &\leq \Big(\frac{1-\eta}{\Delta(\eta)} + \frac{\eta T^\eta}{\Delta(\eta)\Gamma(\eta)}\Big) M_2 d\Big(\widetilde{E}_1(\iota), \widetilde{E}_2(\iota)\Big), \\ d\Big(Z\Big(\widetilde{I}_1(\iota)\Big), Z\Big(\widetilde{I}_2(\iota)\Big)\Big) &\leq \Big(\frac{1-\eta}{\Delta(\eta)} + \frac{\eta T^\eta}{\Delta(\eta)\Gamma(\eta)}\Big) M_3 d\Big(\widetilde{I}_1(\iota), \widetilde{I}_2(\iota)\Big), \\ d\Big(Z\Big(\widetilde{R}_1(\iota)\Big), Z\Big(\widetilde{R}_2(\iota)\Big)\Big) &\leq \Big(\frac{1-\eta}{\Delta(\eta)} + \frac{\eta T^\eta}{\Delta(\eta)\Gamma(\eta)}\Big) M_4 d\Big(\widetilde{R}_1(\iota), \widetilde{R}_2(\iota)\Big), \end{aligned}$$

where $\Big(\frac{1-\eta}{\Delta(\eta)} + \frac{\eta T^\eta}{\Delta(\eta)\Gamma(\eta)}\Big) M_k = L_k < 1, k = 1,2,3,4$ are Lipschitz constants. This means the operator Z is a contraction operator on $C^F(\mathcal{J}, \mathbb{R}) \cap L^F(\mathcal{J}, \mathbb{R})$. Therefore, based on the Banach fixed-point theorem, the model (21) has a unique solution. The same procedure can be used for case (2). □

Remark 3. *It is important to note that the existence of the generalized Hukuhara (gH) difference, which is fundamental to our model's formulation, is implicitly ensured by the conditions of Theorem 2. The Lipschitz condition imposed on functions Fi guarantees that the solutions are sufficiently regular, preventing the diameter of the fuzzy number solutions from shrinking in a way that would invalidate the existence of the gH-difference. Therefore, the conditions for the uniqueness of the solution also serve to ensure the well-posedness of the fuzzy derivatives used in the model.*

5.2. Disease-Free Equilibrium (DFE)

The DFE in the fuzzy context represents a state where the population compartments associated with the disease ($\widetilde{E}$ and $\widetilde{I}$) are effectively zero. Setting $\widetilde{E}(\iota) = \widetilde{0}$ and $\widetilde{I}(\iota) = \widetilde{0}$ in the fuzzy fractional system (19), the Disease-Free Equilibrium for the fuzzy fractional system is the crisp point:

$$\widetilde{P} = \left(\left[\frac{\Theta}{\delta_1}, \frac{\Theta}{\delta_1} \right], [0,0], [0,0], [0,0] \right). \tag{22}$$

The location of the DFE is identical to the crisp integer-order model, represented here as a fuzzy state with zero uncertainty. The fractional order η and the type of gH-differentiability $*$ do not influence the location of this equilibrium, although they would affect its stability analysis.

Remark 4. *The fuzzy fractional system* (19) *possesses the same crisp endemic equilibrium point as the classical model, provided* $\mathcal{R}_0 > 1$. *The existence and location of this crisp EE are independent of the fractional order* η *and the choice of gH-differentiability type* ($* \in \{i, ii\}$). *Determining the existence or nature of non-crisp (fuzzy) endemic equilibria would require more advanced analysis specific to fuzzy differential equations.*

6. Numerical Approach

The fuzzy ABC fractional model (21) with continuous fuzzy functions $F_m\left(\iota, \widetilde{S}(\iota), \widetilde{E}(\iota), \widetilde{I}(\iota), \widetilde{R}(\iota)\right)$, $m = 1,2,3,4$, non-negative kernels for all ι, η, and fuzzy number initial values has a fuzzy solution. Applying the AB fractional integral on both sides of the model (21), we have the following:

$$\begin{cases} {}^{AB}I_0^{\eta}\left({}_0^{ABC}D_{\iota}^{*_1,\eta}\widetilde{S}(\iota)\right) = {}^{AB}I_0^{\eta}F_1\left(\iota, \widetilde{S}(\iota)\right), \\ {}^{AB}I_0^{\eta}\left({}_0^{ABC}D_{\iota}^{*_2,\eta}\widetilde{E}(\iota)\right) = {}^{AB}I_0^{\eta}F_2\left(\iota, \widetilde{E}(\iota)\right), \\ {}^{AB}I_0^{\eta}\left({}_0^{ABC}D_{\iota}^{*_3,\eta}\widetilde{I}(\iota)\right) = {}^{AB}I_0^{\eta}F_3\left(\iota, \widetilde{I}(\iota)\right), \\ {}^{AB}I_0^{\eta}\left({}_0^{ABC}D_{\iota}^{*_4,\eta}\widetilde{R}(\iota)\right) = {}^{AB}I_0^{\eta}F_4\left(\iota, \widetilde{R}(\iota)\right). \end{cases} \tag{23}$$

Now, different cases occur when solving the model (23). To numerically solve the fuzzy fractional model and generate the uncertainty bands shown in the figures, we first transform the fuzzy initial value problem into a system of fractional ordinary differential equations. For a given fuzzy number, its r-cut (or β-cut as used in this paper) is an interval defined by its lower and upper bounds. The fuzzy fractional differential equation system (19) is, therefore, decomposed into a system of eight coupled fractional differential equations, one for the lower bound and one for the upper bound of each of the four state variables (S, E, I, R). We then apply the fractional Adams–Bashforth numerical scheme, as detailed in Equation (26), to this system. The fuzzy initial conditions and parameters (Table 3) are represented as triangular fuzzy numbers, and their interval forms are used in the computation. The resulting lower and upper bound solutions for each compartment are plotted over time. The shaded region between these two bounds represents the fuzzy uncertainty band for a specific r-level (in our figures, r is implicitly set to 1.0 at the peak of the triangular fuzzy number, with the spread shown by the interval). This band visualizes the range of all possible trajectories of the epidemic, given the initial uncertainty in the parameters.

- Case 1: $*_1, *_2, *_3, *_4 = i$.
  In this case, according to Theorem 1 [31], the model (23) gives

$$\begin{cases} \widetilde{S}(\iota) = \widetilde{S}_0 \oplus \frac{1-\eta}{\Delta(\eta)} \odot F_1\Big(\iota, \widetilde{S}(\iota), \widetilde{E}(\iota), \widetilde{I}(\iota), \widetilde{R}(\iota)\Big) \oplus \frac{\eta}{\Delta(\eta)\Gamma(\eta)} \\ \quad \odot \int_0^{\iota} (\iota-\varsigma)^{\eta-1} \odot F_1\Big(\varsigma, \widetilde{S}(\varsigma), \widetilde{E}(\varsigma), \widetilde{I}(\varsigma), \widetilde{R}(\varsigma)\Big) d\varsigma, \\ \widetilde{E}(\iota) = \widetilde{E}_0 \oplus \frac{1-\eta}{\Delta(\eta)} \odot F_2\Big(\iota, \widetilde{S}(\iota), \widetilde{E}(\iota), \widetilde{I}(\iota), \widetilde{R}(\iota)\Big) \oplus \frac{\eta}{\Delta(\eta)\Gamma(\eta)} \\ \quad \odot \int_0^{\iota} (\iota-\varsigma)^{\eta-1} \odot F_2\Big(\varsigma, \widetilde{S}(\varsigma), \widetilde{E}(\varsigma), \widetilde{I}(\varsigma), \widetilde{R}(\varsigma)\Big) d\varsigma, \\ \widetilde{I}(\iota) = \widetilde{I}_0 \oplus \frac{1-\eta}{\Delta(\eta)} \odot F_3\Big(\iota, \widetilde{S}(\iota), \widetilde{E}(\iota), \widetilde{I}(\iota), \widetilde{R}(\iota)\Big) \oplus \frac{\eta}{\Delta(\eta)\Gamma(\eta)} \\ \quad \odot \int_0^{\iota} (\iota-\varsigma)^{\eta-1} \odot F_3\Big(\varsigma, \widetilde{S}(\varsigma), \widetilde{E}(\varsigma), \widetilde{I}(\varsigma), \widetilde{R}(\varsigma)\Big) d\varsigma, \\ \widetilde{R}(\iota) = \widetilde{R}_0 \oplus \frac{1-\eta}{\Delta(\eta)} \odot F_4\Big(\iota, \widetilde{S}(\iota), \widetilde{E}(\iota), \widetilde{I}(\iota), \widetilde{R}(\iota)\Big) \oplus \frac{\eta}{\Delta(\eta)\Gamma(\eta)} \\ \quad \odot \int_0^{\iota} (\iota-\varsigma)^{\eta-1} \odot F_4\Big(\varsigma, \widetilde{S}(\varsigma), \widetilde{E}(\varsigma), \widetilde{I}(\varsigma), \widetilde{R}(\varsigma)\Big) d\varsigma. \end{cases}$$

Putting $\iota = \iota_n = 0 + nh$, where h is a constant step-size, the following is obtained:

$$\begin{cases} \widetilde{S}(\iota_n) = \widetilde{S}_0 \oplus \frac{1-\eta}{\Delta(\eta)} \odot F_1\Big(\iota_n, \widetilde{S}(\iota_n), \widetilde{E}(\iota_n), \widetilde{I}(\iota_n), \widetilde{R}(\iota_n)\Big) \oplus \frac{\eta}{\Delta(\eta)\Gamma(\eta)} \\ \quad \odot \sum_{i=1}^{n-1} \int_{\iota_i}^{\iota_{i+1}} (\iota_n-\varsigma)^{\eta-1} \odot F_1\Big(\varsigma, \widetilde{S}(\varsigma), \widetilde{E}(\varsigma), \widetilde{I}(\varsigma), \widetilde{R}(\varsigma)\Big) d\varsigma, \\ \widetilde{E}(\iota_n) = \widetilde{E}_0 \oplus \frac{1-\eta}{\Delta(\eta)} \odot F_2\Big(\iota_n, \widetilde{S}(\iota_n), \widetilde{E}(\iota_n), \widetilde{I}(\iota_n), \widetilde{R}(\iota_n)\Big) \oplus \frac{\eta}{\Delta(\eta)\Gamma(\eta)} \\ \quad \odot \sum_{i=1}^{n-1} \int_{\iota_i}^{\iota_{i+1}} (\iota_n-\varsigma)^{\eta-1} \odot F_2\Big(\varsigma, \widetilde{S}(\varsigma), \widetilde{E}(\varsigma), \widetilde{I}(\varsigma), \widetilde{R}(\varsigma)\Big) d\varsigma, \\ \widetilde{I}(\iota_n) = \widetilde{I}_0 \oplus \frac{1-\eta}{\Delta(\eta)} \odot F_3\Big(\iota_n, \widetilde{S}(\iota_n), \widetilde{E}(\iota_n), \widetilde{I}(\iota_n), \widetilde{R}(\iota_n)\Big) \oplus \frac{\eta}{\Delta(\eta)\Gamma(\eta)} \\ \quad \odot \sum_{i=1}^{n-1} \int_{\iota_i}^{\iota_{i+1}} (\iota_n-\varsigma)^{\eta-1} \odot F_3\Big(\varsigma, \widetilde{S}(\varsigma), \widetilde{E}(\varsigma), \widetilde{I}(\varsigma), \widetilde{R}(\varsigma)\Big) d\varsigma, \\ \widetilde{R}(\iota_n) = \widetilde{R}_0 \oplus \frac{1-\eta}{\Delta(\eta)} \odot F_4\Big(\iota_n, \widetilde{S}(\iota_n), \widetilde{E}(\iota_n), \widetilde{I}(\iota_n), \widetilde{R}(\iota_n)\Big) \oplus \frac{\eta}{\Delta(\eta)\Gamma(\eta)} \\ \quad \odot \sum_{i=1}^{n-1} \int_{\iota_i}^{\iota_{i+1}} (\iota_n-\varsigma)^{\eta-1} \odot F_4\Big(\varsigma, \widetilde{S}(\varsigma), \widetilde{E}(\varsigma), \widetilde{I}(\varsigma), \widetilde{R}(\varsigma)\Big) d\varsigma. \end{cases} \tag{24}$$

Now, we approximate the function $F_l\Big(\varsigma, \widetilde{S}(\varsigma), \widetilde{E}(\varsigma), \widetilde{I}(\varsigma), \widetilde{R}(\varsigma)\Big), l = 1,2,3,4$ on the interval $[\iota_i, \iota_{i+1}]$ by the Lagrange interpolation as follows:

$$\begin{cases} F_l\Big(\varsigma, \widetilde{S}(\varsigma), \widetilde{E}(\varsigma), \widetilde{I}(\varsigma), \widetilde{R}(\varsigma)\Big) \simeq F_l\Big(\iota_{i+1}, \widetilde{S}(\iota_{i+1}), \widetilde{E}(\iota_{i+1}), \widetilde{I}(\iota_{i+1}), \widetilde{R}(\iota_{i+1})\Big) \\ \oplus \left[\frac{\varsigma-\iota_{i+1}}{h} \left(\ominus(-1) \left[\begin{array}{c} F_l\Big(\iota_{i+1}, \widetilde{S}(\iota_{i+1}), \widetilde{E}(\iota_{i+1}), \widetilde{I}(\iota_{i+1}), \widetilde{R}(\iota_{i+1})\Big) \\ \ominus F_l\Big(\iota_i, \widetilde{S}(\iota_i), \widetilde{E}(\iota_i), \widetilde{I}(\iota_i), \widetilde{R}(\iota_i)\Big) \end{array}\right]\right)\right], \varsigma \in [\iota_i, \iota_{i+1}]. \end{cases} \tag{25}$$

By substituting (25) in model (24) with some algebraic operations, we obtain

$$\begin{cases} \widetilde{S}(\iota_n) = \widetilde{S}_0 \oplus \frac{\eta h^{\eta}}{\Delta(\eta)} \odot \left[\begin{array}{c} \varepsilon_n \odot F_1\Big(0, \widetilde{S}(0), \widetilde{E}(0), \widetilde{I}(0), \widetilde{R}(0)\Big) \\ \oplus \sum_{i=1}^{n} \mu_{n-i} F_1\Big(\iota_i, \widetilde{S}(\iota_i), \widetilde{E}(\iota_i), \widetilde{I}(\iota_i), \widetilde{R}(\iota_i)\Big) \end{array}\right], \\ \widetilde{E}(\iota_n) = \widetilde{E}_0 \oplus \frac{\eta h^{\eta}}{\Delta(\eta)} \odot \left[\begin{array}{c} \varepsilon_n \odot F_2\Big(0, \widetilde{S}(0), \widetilde{E}(0), \widetilde{I}(0), \widetilde{R}(0)\Big) \\ \oplus \sum_{i=1}^{n} \mu_{n-i} F_2\Big(\iota_i, \widetilde{S}(\iota_i), \widetilde{E}(\iota_i), \widetilde{I}(\iota_i), \widetilde{R}(\iota_i)\Big) \end{array}\right], \\ \widetilde{I}(\iota_n) = \widetilde{I}_0 \oplus \frac{\eta h^{\eta}}{\Delta(\eta)} \odot \left[\begin{array}{c} \varepsilon_n \odot F_3\Big(0, \widetilde{S}(0), \widetilde{E}(0), \widetilde{I}(0), \widetilde{R}(0)\Big) \\ \oplus \sum_{i=1}^{n} \mu_{n-i} F_3\Big(\iota_i, \widetilde{S}(\iota_i), \widetilde{E}(\iota_i), \widetilde{I}(\iota_i), \widetilde{R}(\iota_i)\Big) \end{array}\right], \\ \widetilde{R}(\iota_n) = \widetilde{R}_0 \oplus \frac{\eta h^{\eta}}{\Delta(\eta)} \odot \left[\begin{array}{c} \varepsilon_n \odot F_4\Big(0, \widetilde{S}(0), \widetilde{E}(0), \widetilde{I}(0), \widetilde{R}(0)\Big) \\ \oplus \sum_{i=1}^{n} \mu_{n-i} F_4\Big(\iota_i, \widetilde{S}(\iota_i), \widetilde{E}(\iota_i), \widetilde{I}(\iota_i), \widetilde{R}(\iota_i)\Big) \end{array}\right], \end{cases} \tag{26}$$

where

$$\Delta(\eta) = 1 - \eta + \frac{\eta}{\Gamma(\eta)}, \tag{27}$$

$$\varepsilon_n = \frac{(n-1)^{\eta+1} - n^{\eta}(n-\eta-1)}{\Gamma(\eta+2)}, \tag{28}$$

and

$$\mu_k = \begin{cases} \frac{1}{\Gamma(\eta+2)} + \frac{1-\eta}{\eta h^{\eta}}, k = 0, \\ \frac{(k-1)^{\eta-1} - 2k^{\eta+1} + (k+1)^{\eta+1}}{\Gamma(\eta+2)}, k = 1, 2, ..., n-1. \end{cases} \tag{29}$$

According to values of the parameters as presented in Table 3, we will plot the Figures 1–7 of the solutions in case 1 with different fractional order $\eta = 0.3, 0.4, 0.5, 0.6, 0.7, 0.8, 0.9$.

Table 3. The model parameters and their values.

Parameter	Numerical Estimation
δ_0	0.001
δ_1	0.001
δ_2	$[0.9 + 0.08r, 1 - 0.2r]$
δ_3	$[0.7 + 0.08r, 0.9 - 0.12r]$
δ_4	$[0.6 + 0.02r, 0.8 - 0.18r]$
S_0	$[17.7 + 0.3r, 18.2 - 0.2r]$
E_0	$[9.5 + 0.5r, 10.3 - 0.3r]$
I_0	$[6.8 + 0.2r, 7.3 - 0.3r]$
R_0	$[4.9 + 0.1r, 5.2 - 0.2r]$

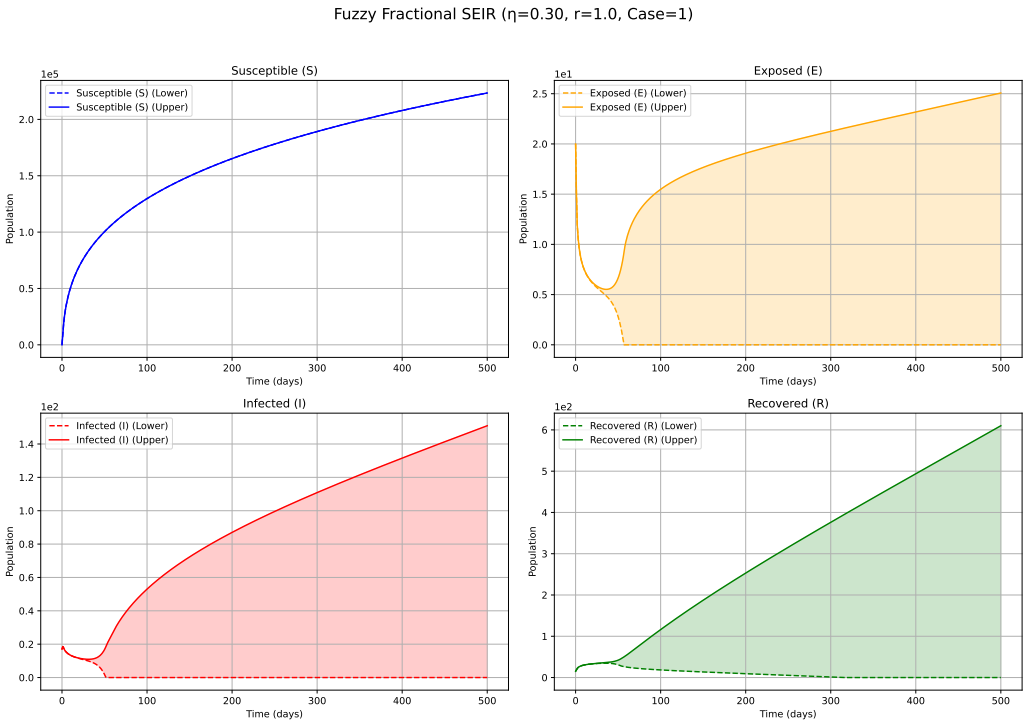

Figure 1. Fuzzy solutions of susceptible, Exposed, Infected, and Recovered classes in case (i)-gH with order $\eta = 0.30$.

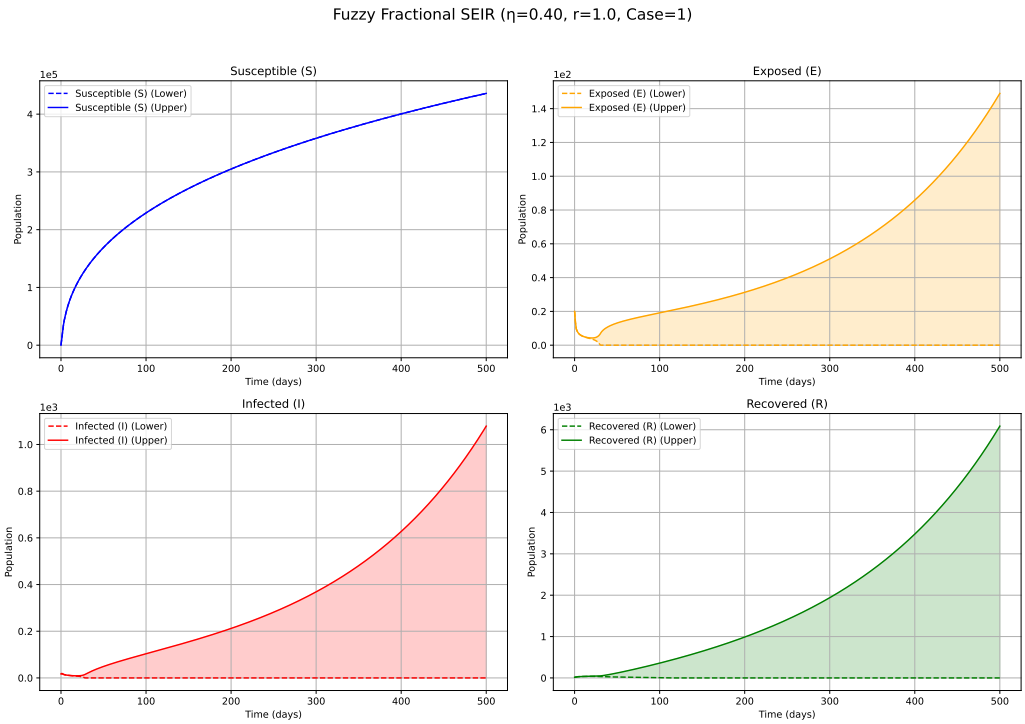

Figure 2. Fuzzy solutions of susceptible, Exposed, Infected, and Recovered classes in case (i)-gH with order $\eta = 0.40$.

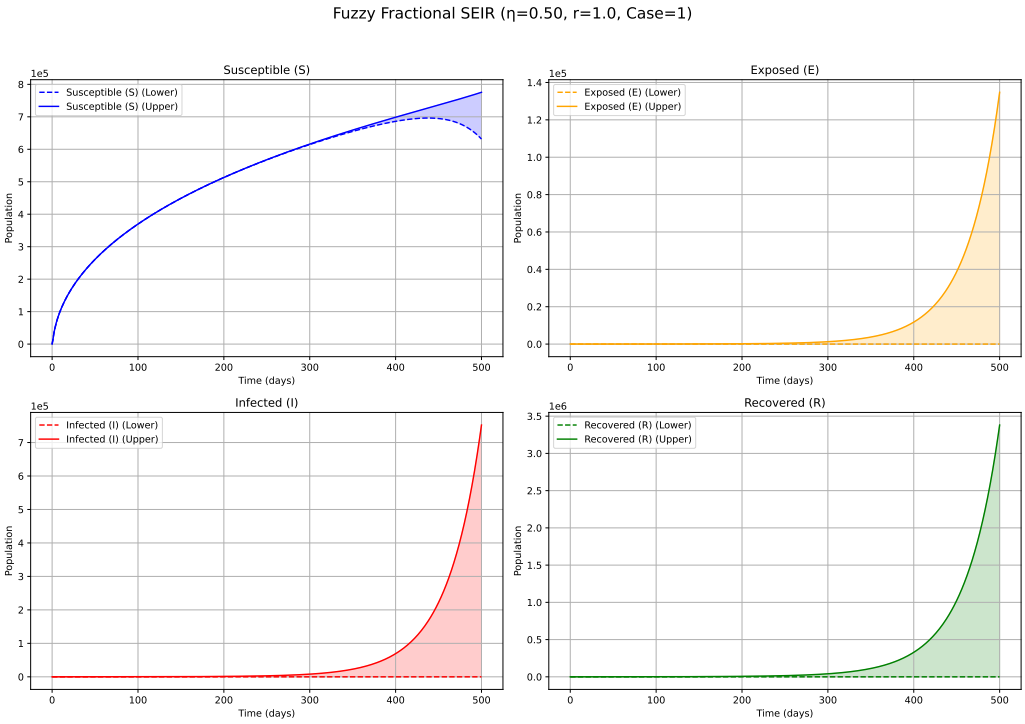

Figure 3. Fuzzy solutions of susceptible, Exposed, Infected, and Recovered classes in case (i)-gH with order $\eta = 0.50$.

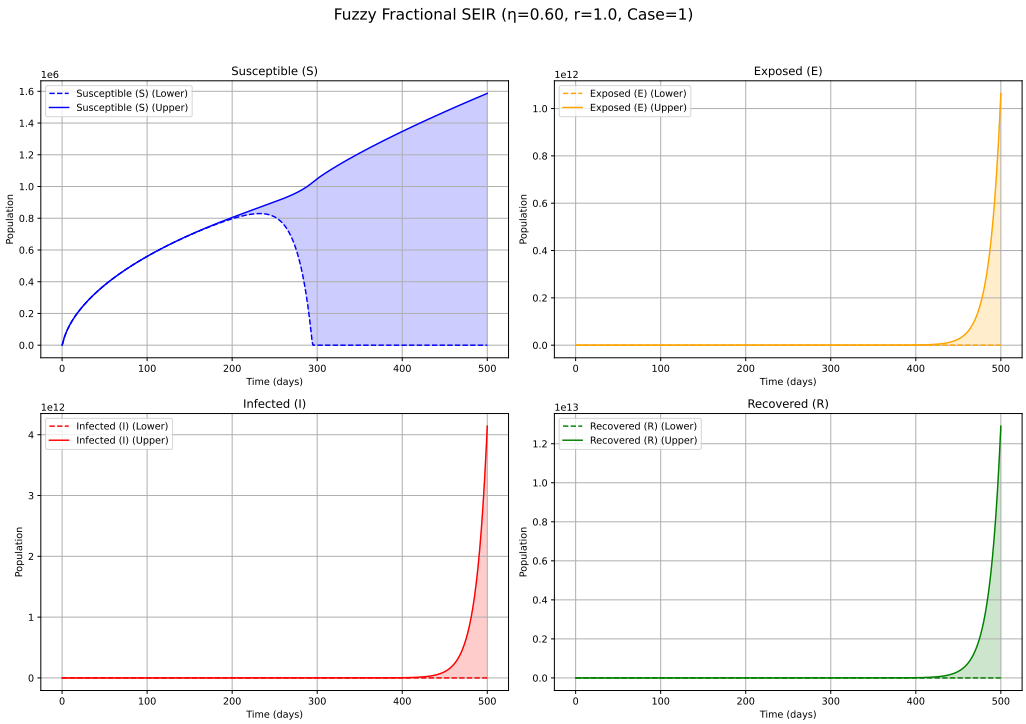

Figure 4. Fuzzy solutions of susceptible, Exposed, Infected, and Recovered classes in case (i)-gH with order $\eta = 0.60$.

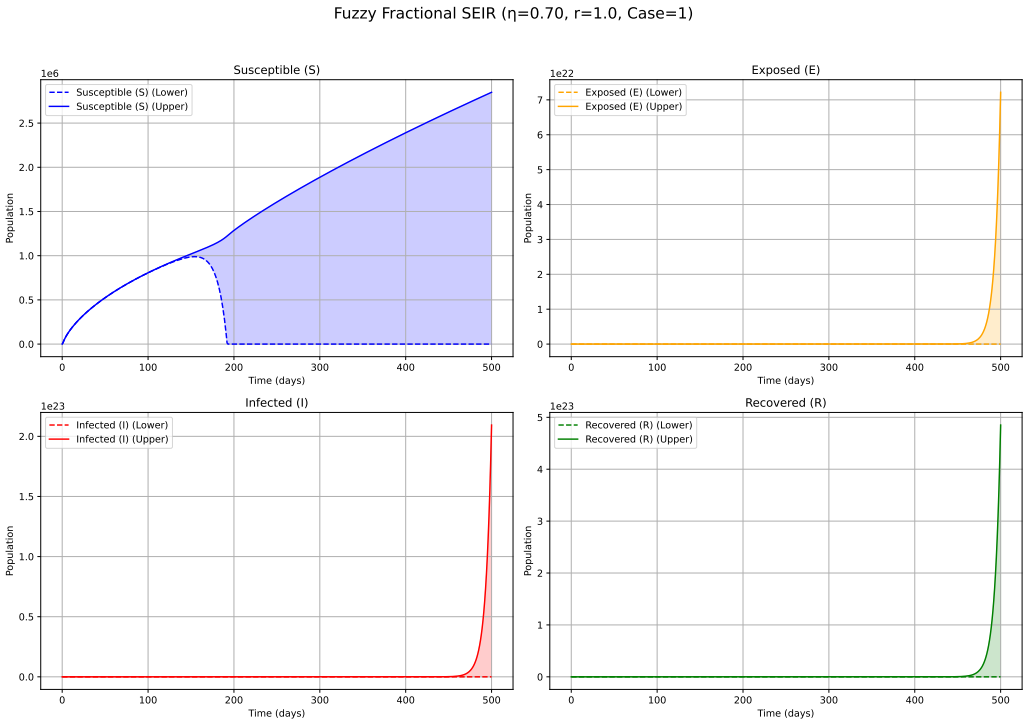

Figure 5. Fuzzy solutions of susceptible, Exposed, Infected, and Recovered classes in case (i)-gH with order $\eta = 0.70$.

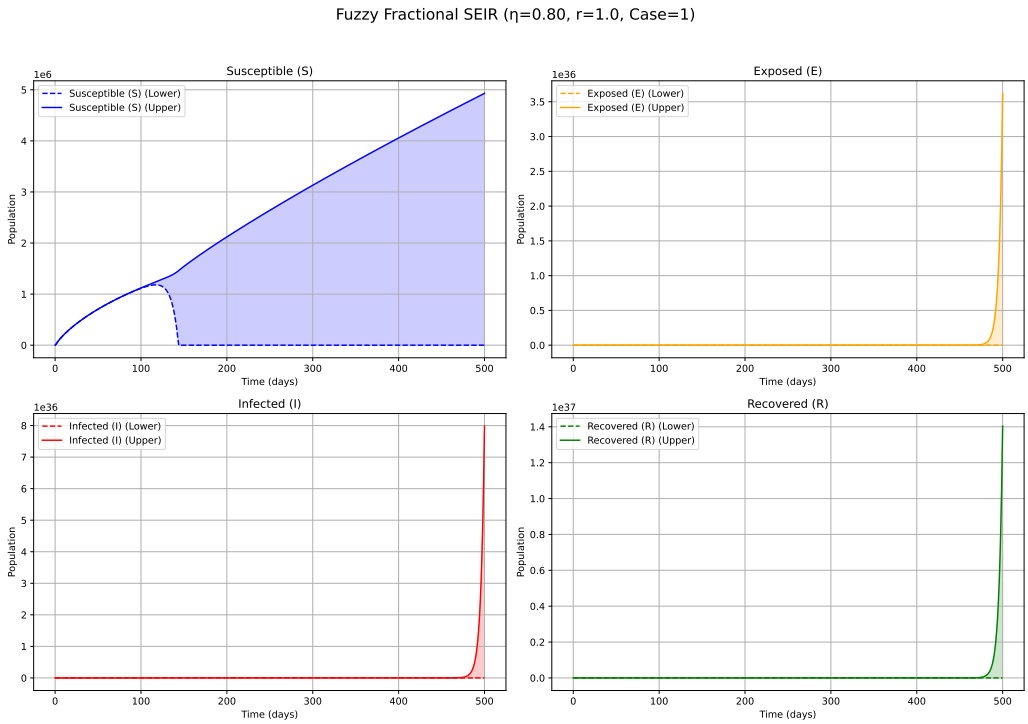

Figure 6. Fuzzy solutions of susceptible, Exposed, Infected, and Recovered classes in case (i)-gH with order $\eta = 0.80$.

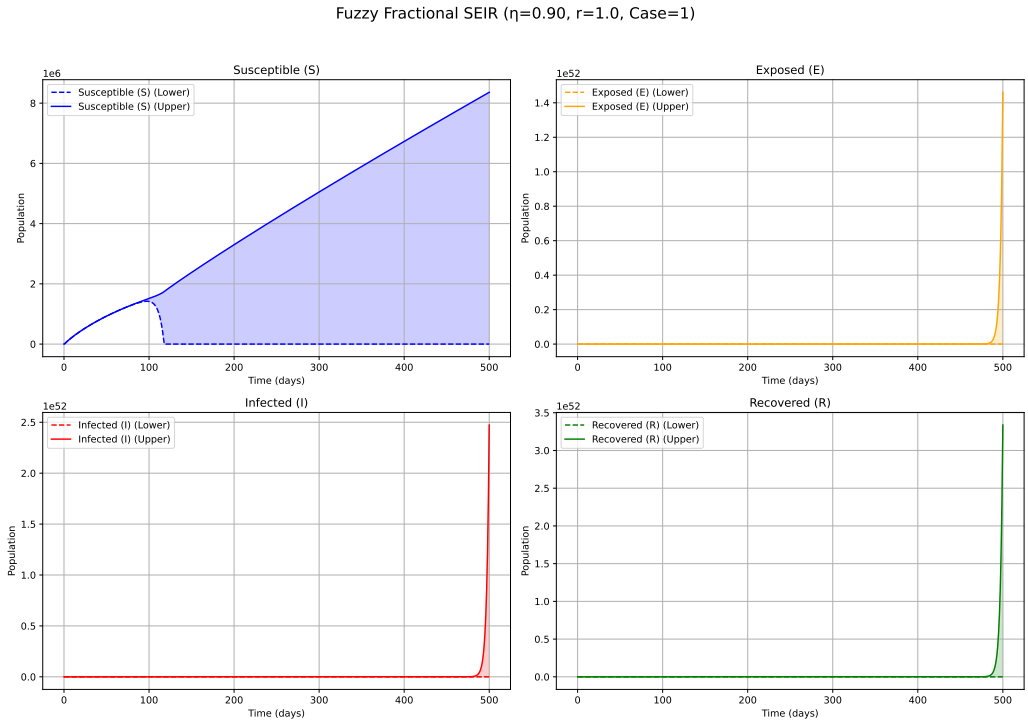

Figure 7. Fuzzy solutions of susceptible, Exposed, Infected, and Recovered classes in case (i)-gH with order $\eta = 0.90$.

- Case 2: $*_1, *_2, *_3, *_4 = ii$.
  In this case, the solution of model (23) can be achieved similarly to the previous case by solving the following model:

$$\begin{cases} \ominus(-1)\widetilde{S}(\iota_n) = \ominus(-1)\widetilde{S}_0 \oplus \frac{\eta h^\eta}{\Delta(\eta)} \odot \begin{bmatrix} \varepsilon_n \odot F_1\left(0, \widetilde{S}(0), \widetilde{E}(0), \widetilde{I}(0), \widetilde{R}(0)\right) \\ \oplus \sum_{i=1}^{n} \mu_{n-i} F_1\left(\iota_i, \widetilde{S}(\iota_i), \widetilde{E}(\iota_i), \widetilde{I}(\iota_i), \widetilde{R}(\iota_i)\right) \end{bmatrix}, \\ \ominus(-1)\widetilde{E}(\iota_n) = \ominus(-1)\widetilde{E}_0 \oplus \frac{\eta h^\eta}{\Delta(\eta)} \odot \begin{bmatrix} \varepsilon_n \odot F_2\left(0, \widetilde{S}(0), \widetilde{E}(0), \widetilde{I}(0), \widetilde{R}(0)\right) \\ \oplus \sum_{i=1}^{n} \mu_{n-i} F_2\left(\iota_i, \widetilde{S}(\iota_i), \widetilde{E}(\iota_i), \widetilde{I}(\iota_i), \widetilde{R}(\iota_i)\right) \end{bmatrix}, \\ \ominus(-1)\widetilde{I}(\iota_n) = \ominus(-1)\widetilde{I}_0 \oplus \frac{\eta h^\eta}{\Delta(\eta)} \odot \begin{bmatrix} \varepsilon_n \odot F_3\left(0, \widetilde{S}(0), \widetilde{E}(0), \widetilde{I}(0), \widetilde{R}(0)\right) \\ \oplus \sum_{i=1}^{n} \mu_{n-i} F_3\left(\iota_i, \widetilde{S}(\iota_i), \widetilde{E}(\iota_i), \widetilde{I}(\iota_i), \widetilde{R}(\iota_i)\right) \end{bmatrix}, \\ \ominus(-1)\widetilde{R}(\iota_n) = \ominus(-1)\widetilde{R}_0 \oplus \frac{\eta h^\eta}{\Delta(\eta)} \odot \begin{bmatrix} \varepsilon_n \odot F_4\left(0, \widetilde{S}(0), \widetilde{E}(0), \widetilde{I}(0), \widetilde{R}(0)\right) \\ \oplus \sum_{i=1}^{n} \mu_{n-i} F_4\left(\iota_i, \widetilde{S}(\iota_i), \widetilde{E}(\iota_i), \widetilde{I}(\iota_i), \widetilde{R}(\iota_i)\right) \end{bmatrix}, \end{cases} \tag{30}$$

We will plot the Figures 8–11 of the solutions in case 2 with different fractional order η.

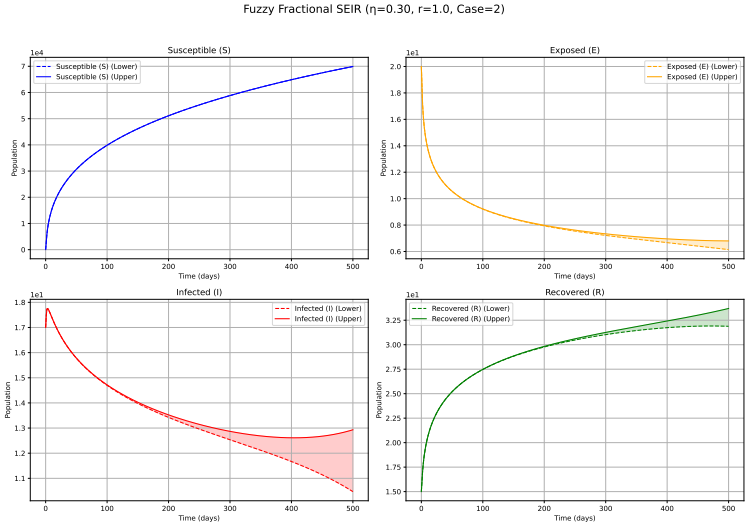

Figure 8. Fuzzy solutions of susceptible, Exposed, Infected, and Recovered classes in case (ii)-gH with order $\eta = 0.30$.

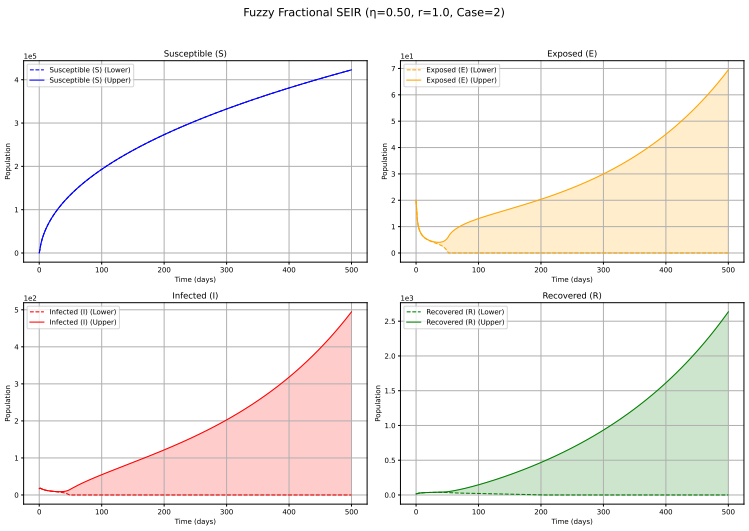

Figure 9. Fuzzy solutions of susceptible, Exposed, Infected, and Recovered classes in case (ii)-gH with order $\eta = 0.50$.

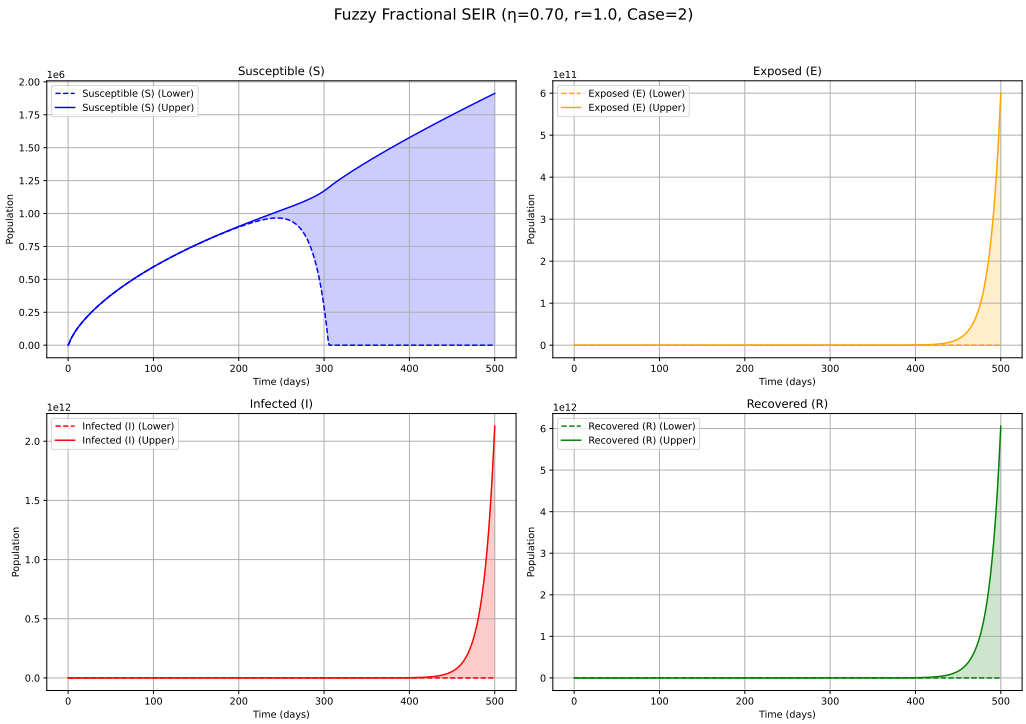

Figure 10. Fuzzy solutions of susceptible, Exposed, Infected, and Recovered classes in case (ii)-gH with order $\eta = 0.70$.

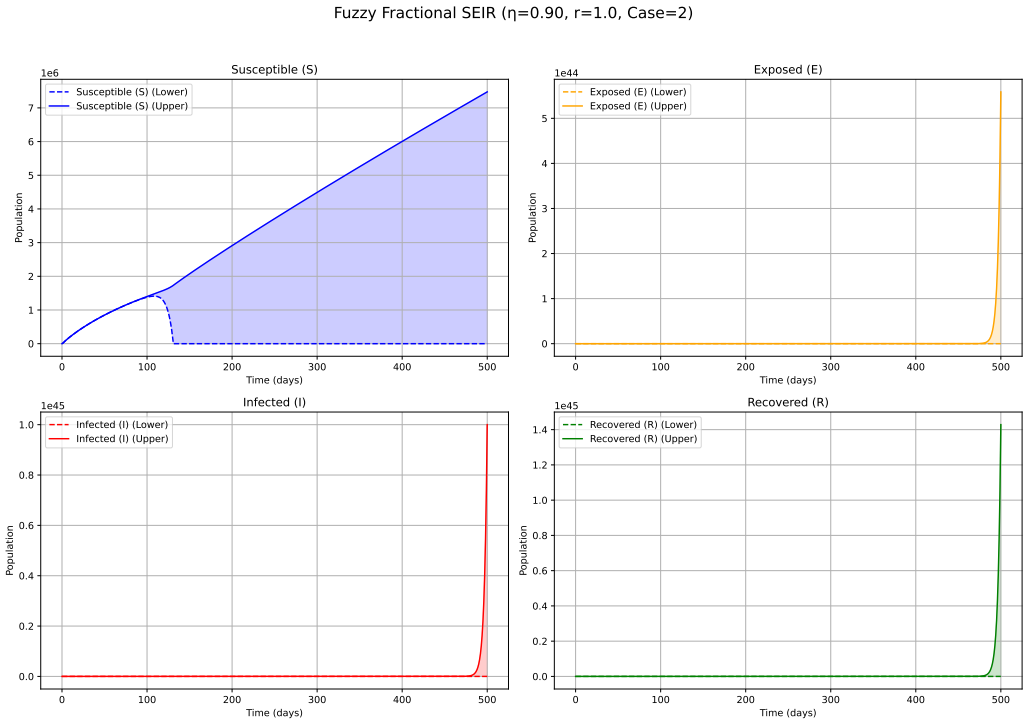

Figure 11. Fuzzy solutions of susceptible, Exposed, Infected, and Recovered classes in case (ii)-gH with order $\eta = 0.90$.

7. Biological Significance and Interpretation of Figures

The numerical simulations, visualized in Figures 1–11, demonstrate the temporal propagation of uncertainty, quantified by the width of the fuzzy bands encompassing the state variable trajectories. Furthermore, these figures elucidate the significant influence of

both the fractional order (η) and the choice of generalized Hukuhara (gH) differentiability (Case 1: $(i)-gH$ vs. Case 2: $(ii)-gH$) on the resultant epidemic dynamics. Impact of Fractional Order (η)—Case 1 ($(i)-gH$ Differentiability; Figures 1–7, Table 4): The fractional order η serves as an index of system memory, modulating the extent to which past states influence future epidemic progression. Low η values (e.g., 0.3, 0.4; Figures 1 and 2): Diminishing values of η signify heightened memory effects, wherein the system's past states exert a more substantial influence on current and future dynamics. Biologically, such scenarios may reflect the impact of factors like prolonged immunity, persistent environmental viral reservoirs (e.g., the virus surviving for a time on surfaces or in contaminated water sources), or slowly evolving public health behaviors. Consequently, the simulated epidemic curves for Exposed (E) and Infected (I) compartments display attenuated, wider peaks, characteristic of a protracted epidemic wave and a more pronounced "flattening of the curve." The associated fuzzy bands, representing uncertainty, also tend to remain wider for extended periods, indicating sustained uncertainty under strong memory conditions. Medium η values (e.g., 0.5, 0.6, 0.7; Figures 3–5): Intermediate η values represent a transitional regime with moderate memory effects. The epidemic wave becomes more distinctly defined compared with low η scenarios, featuring earlier and comparatively sharper peaks, indicating a tempered influence of historical system states on the epidemiological trajectory. High η values (e.g., 0.8, 0.9, approaching 1; Figures 6 and 7): Conversely, higher η values lead to system dynamics that increasingly resemble those of classical integer-order models, characterized by diminished memory effects. Epidemics under these conditions progress more rapidly, exhibit sharper and higher incidence peaks, and resolve more quickly, reflecting a greater responsiveness to contemporaneous conditions. The fuzzy uncertainty bands may also converge more rapidly as the system's trajectory becomes more deterministic.

Table 4. Summary of Fuzzy Fractional SEIR Model solutions for Case 1 (all derivatives Type 'i') at different fractional orders (η).

Fractional Order (η)	General Trend in Compartments (Visual)	Key Biological Interpretation
Low η (e.g., 0.3, 0.4)	S: Slow decline, eventual slow recovery. E, I: Lower, broader peaks; epidemic wave delayed and spread out. R: Slow accumulation.	Strong Memory Effects: Past states heavily influence current dynamics. Slower Epidemic: Disease spreads slowly, prolonged duration, less intense peak. Delayed Response: System and interventions may show delayed effects. Sustained Uncertainty: Fuzzy bands (uncertainty) tend to be wider for longer.
Medium η (e.g., 0.5, 0.6, 0.7)	S: More pronounced decline and recovery phases. E, I: Peaks are higher and occur earlier than for low η; epidemic wave is more defined. R: Faster accumulation.	Moderate Memory Effects: System history influences dynamics, but less dominantly. Balanced Dynamics: Represents a transition between slow memory-laden and faster classical dynamics. "Flattening of the curve" effect still noticeable.
High η (e.g., 0.8, 0.9, $\rightarrow$ 1)	S: Faster decline, sharper "dip" possible. E, I: Sharper, higher peaks occurring earlier; epidemic wave more compressed. R: Rapid accumulation.	Weak Memory Effects: System behaves more like a classical integer-order model. Faster Epidemic: Disease spreads more rapidly, leading to a more intense and shorter epidemic. Quicker Response: System responds quickly to current conditions.

Impact of Derivative Type—Case 2 ($(ii)-gH$ Differentiability; Figures 8–11, Table 5): The selection of gH-differentiability profoundly alters the interpretation of the fuzzy system's evolution, particularly for the Exposed (E) and Infected (I) compartments. Low η values (e.g., 0.3; Figure 8): Under $(ii)-gH$ differentiability, particularly at low η values, the system demonstrates pronounced memory retention and sluggish dynamics. Notably, for the E and I compartments, instead of a distinct outbreak peak as observed in Case 1, a slow, monotonic decline from initial fuzzy values is observed. This suggests a dynamic dominated by disease fade-out or a very gradual transition towards an equilibrium state, without the emergence of a significant new infection wave. The historical states heavily influence this slow decay, with new infection generation being insufficient to trigger a resurgence within the simulation period. Higher η values (e.g., 0.7, 0.9; Figures 10 and 11): As η increases within Case 2, the rate of this decay or stabilization accelerates. However, the fundamental characteristic of not producing a new prominent outbreak peak (for E and I compartments, unlike in Case 1) persists. The system continues to reflect a decay or stabilization trajectory, though with a progressively weaker influence of past states compared with lower η values in this differentiability case. The contrasting dynamics between Case 1 and Case 2 underscore the nuanced complexities introduced by the fuzzy fractional framework. Case 1 ($(i)-gH$) dynamics are generally consistent with the canonical pattern of active epidemic propagation followed by decline. In contrast, Case 2 ($(ii)-gH$) dynamics, especially for the E and I compartments may represent scenarios where initial conditions or parameterizations favor direct decay or slow convergence towards an equilibrium. This behavior could be attributed to the specific mathematical properties of $(ii)-gH$ differentiability when applied to the model's governing equations and the way it interacts with the fuzzy representation of state variables. This distinction is of paramount importance for epidemiological modeling, as the choice of gH-differentiability can lead to qualitatively disparate predictions regarding the emergence and characteristics of future epidemic waves.

Table 5. Summary of Fuzzy Fractional SEIR model solutions for Case 2 (all derivatives Type 'ii') at different fractional orders (η).

Fractional Order (η)	General Trend in Compartments (Visual)	Key Biological Interpretation
Low η (e.g., 0.3)	S: Very slow, monotonic evolution (decline or slight increase). E, I: Very slow, monotonic decline from initial fuzzy values. No distinct new outbreak peak. R: Very slow, monotonic increase.	Very Strong Memory and Sluggish Dynamics: System evolution is extremely slow under this type of differentiability. Decay/Stabilization Phase: Suggests a scenario of disease fade-out or slow transition to equilibrium, rather than an active outbreak. Past Dominance: Past states heavily dictate the very slow current transitions.
High η (e.g., 0.9, $\rightarrow 1$)	S: Faster monotonic evolution compared to low η. E, I: Faster monotonic decline from initial fuzzy values. R: Faster monotonic increase.	Moderate Memory, Faster Transition: System still shows decay/stabilization but transitions more quickly. Reduced Influence of Past: While memory is present, the system moves towards its equilibrium state more rapidly than with low η. Still no new outbreak peak.

From a public health perspective, the interval-valued solutions generated by this fuzzy fractional framework offer significant advantages for decision-making under uncertainty. Instead of providing a single, deterministic prediction for the epidemic's peak or duration,

the model provides a range of possibilities encapsulated within the fuzzy bands. This allows authorities to engage in more robust planning. For example, the upper bound of the infected compartment's trajectory can inform worst-case scenario planning for hospital bed capacity, while the lower bound can help establish a baseline for resource allocation. The width of the fuzzy band itself is a quantitative measure of predictive uncertainty. A wider band might prompt decision-makers to adopt more flexible, adaptive strategies or to invest in better data collection to reduce uncertainty. Thus, these fuzzy results can be used to formulate more resilient public health policies for vaccination campaigns, resource stockpiling, and risk communication that account for the inherent unpredictability of epidemic dynamics.

8. Conclusions

In this work, we have developed and analyzed an SEIR influenza epidemic model incorporating fuzzy Atangana–Baleanu–Caputo (ABC) fractional derivatives and a Crowley–Martin incidence rate. This approach uniquely combines the ability to represent inherent uncertainties in epidemiological parameters and state variables (through fuzzy numbers) with the capacity to model memory effects and non-local dynamics (through fractional calculus). The Crowley–Martin incidence rate is included to provide a more flexible mechanism that can potentially enhance realism by accounting for saturation effects at high densities of susceptible or infectious individuals. The SEIR model with Crowley–Martin incidence and ABC fractional derivatives provides a flexible framework for studying disease dynamics. Key properties, such as positivity and boundedness, ensure biological relevance. The basic reproduction number $\mathcal{R}_0$ acts as a threshold: the DFE is locally stable if $\mathcal{R}_0 < 1$ and unstable if $\mathcal{R}_0 > 1$. An endemic equilibrium may exist and be stable if $\mathcal{R}_0 > 1$. The fractional order η and the fuzzy nature of the derivatives/parameters add significant complexity to the analysis, requiring specialized mathematical tools, but offer the potential for a more realistic description of real-world epidemic processes with memory and uncertainty. Numerical simulations are often essential to explore the dynamics of such complex models. This work provides a more nuanced understanding by simultaneously accounting for memory effects and inherent uncertainties. The numerical simulations demonstrate the profound impact of the fractional order and the type of fuzzy differentiability on epidemic trajectories, yielding interval-valued predictions that are more informative for public health decision-making than single-point estimates. This framework lays the groundwork for more sophisticated and realistic epidemiological models that can better capture the complexities of infectious disease spread. However, we acknowledge that the practical validation of this model is a critical next step. Future work should focus on applying this framework to a real-world case study using influenza surveillance data. Such an investigation would involve the complex task of estimating the fuzzy parameters from empirical data and validating the model's interval-valued predictions against observed epidemic trajectories. This would bridge the gap between this theoretical development and its potential application in public health planning and decision-making under uncertainty, thereby demonstrating its full practical utility.

It is important to acknowledge the limitations of the current model, which define avenues for future research. First, our model assumes homogeneous mixing within the population, a common simplification that does not account for spatial or social structures. Second, the analysis relies on parameters from the literature rather than fitting them to a specific epidemiological dataset, a task that would require advanced statistical methods for fuzzy fractional systems. Third, while the ABC fractional derivative provides a sophisticated memory kernel, its specific form may not be optimal for all biological processes. Finally, the complexity of the fuzzy fractional framework itself can be a barrier to direct

implementation by public health agencies. These limitations underscore that our model serves as a foundational step, demonstrating the potential of this approach, rather than a final, universally applicable predictive tool.

Author Contributions: Conceptualization, M.A.; Data curation, A.A.Q.; Formal analysis, F.G., A.A.Q. and E.I.H.; Investigation, M.R. and E.I.H.; Methodology, M.A., M.R., K.A. and A.E.-S.; Project administration, K.A.; Software, F.G.; Supervision, K.A.; Writing—original draft, A.A.Q. and M.A.; Writing—review and editing, F.G., M.A., K.A., A.E.-S. and E.I.H. All authors have read and agreed to the published version of the manuscript.

Funding: This work was supported and funded by the Deanship of Scientific Research at Imam Mohammad Ibn Saud Islamic University (IMSIU) (grant number IMSIU-DDRSP2502).

Data Availability Statement: All data used in this work are contained within the article.

Conflicts of Interest: The author declares that the research was conducted in the absence of any Conflict of interest.

References

1. Past Flu Season Severity Assessments | Influenza (Flu) | CDC. Available online: https://www.cdc.gov/flu/php/surveillance/past-seasons.html (accessed on 17 December 2024).
2. Preliminary Estimated Flu Disease Burden 2023–2024 Flu Season | Flu Burden | CDC. Available online: https://www.cdc.gov/flu-burden/php/data-vis/2023-2024.html (accessed on 17 December 2024).
3. Routine Immunizations on Schedule for Everyone (RISE) | Vaccines & Immunizations | CDC. Available online: https://www.cdc.gov/vaccines/php/rise/index.html (accessed on 31 December 2024).
4. Hamson, E.; Forbes, C.; Wittkopf, P.; Pandey, A.; Mendes, D.; Kowalik, J.; Czudek, C.; Mugwagwa, T. Impact of pandemics and disruptions to vaccination on infectious diseases epidemiology past and present. Hum. *Vaccines Immunother.* **2023**, *19*, 2219577. [CrossRef] [PubMed]
5. Peiris, J.S.M.; de Jong, M.D.; Guan, Y. Avian influenza virus (H5N1): A threat to human health. *Clin. Microbiol. Rev.* **2007**, *20*, 243–267. [CrossRef] [PubMed]
6. Nisar, K.S.; Ahmad, S.; Ullah, A.; Shah, K.; Alrabaiah, H.; Arfan, M. Mathematical analysis of SIRD model of COVID-19 with Caputo fractional derivative based on real data. *Results Phys.* **2021**, *21*, 103772. [CrossRef] [PubMed]
7. Yang, S.; Zhou, Y.; Li, L. Progress on Epidemiology of Influenza A (H1N1). In *Progress in China Epidemiology*; Springer Nature: Singapore, 2023; Volume 1, pp. 33–50.
8. Algolam, M.S.; Almalahi, M.; Aldwoah, K.; Awaad, A.S.; Suhail, M.; Alshammari, F.A.; Younis, B. Theoretical and Numerical Analysis of the SIR Model and Its Symmetric Cases with Power Caputo Fractional Derivative. *Fractal Fract.* **2025**, *9*, 251. [CrossRef]
9. Al-Zahrani, S.M.; Elsmih, F.E.I.; Al-Zahrani, K.S.; Saber, S. A fractional order SITR model for forecasting of transmission of COVID-19: Sensitivity statistical analysis. *Malays. J. Math. Sci.* **2022**, *16*, 517–536. [CrossRef]
10. Aly, E.S.; Almalahi, M.A.; Aldwoah, K.A.; Shah, K. Criteria of existence and stability of an n-coupled system of generalized Sturm-Liouville equations with a modified ABC fractional derivative and an application to the SEIR influenza epidemic model. *AIMS Math.* **2024**, *9*, 14228–14252. [CrossRef]
11. Cori, A.; Valleron, A.; Carrat, F.; Tomba, G.S.; Thomas, G.; Boëlle, P. Estimating influenza latency and infectious period durations using viral excretion data. *Epidemics* **2012**, *4*, 132–138. [CrossRef]
12. Alzahrani, S.M.; Saadeh, R.; Abdoon, M.A.; Qazza, A.; Guma, F.E.; Berir, M. Numerical simulation of an influenza epidemic: Prediction with fractional SEIR and the ARIMA model. *Appl. Math. Inf. Sci.* **2024**, *18*, 1–12.
13. Avilov, K.K.; Li, Q.; Lin, L.; Demirhan, H.; Stone, L.; He, D. The 1978 English boarding school influenza outbreak: Where the classic SEIR model fails. *J. R. Soc. Interface* **2024**, *21*, 20240394. [CrossRef]
14. McKinney, B.; Imran, M.; Butt, A.I.K. SEIR Mathematical Model for Influenza-Corona Co-Infection with Treatment and Hospitalization Compartments and Optimal Control Strategies. *Comput. Model. Eng. Sci.* **2025**, *142*, 1899–1931. [CrossRef]
15. Baleanu, D.; Diethelm, K.; Scalas, E.; Trujillo, J.J. *Fractional Calculus: Models and Numerical Methods*; World Scientific: Singapore, 2012; Volume 3.
16. Petras, I. Fractional calculus and its applications. In *Mathematical Modeling with Multidisciplinary Applications*; John Wiley & Sons: Hoboken, NJ, USA, 2012; pp. 355–396.
17. Dalir, M.; Bashour, M. Applications of fractional calculus. *Appl. Math. Sci.* **2010**, *4*, 1021–1032.
18. Magin, R.L. Fractional calculus models of complex dynamics in biological tissues. *Comput. Math. Appl.* **2010**, *59*, 1586–1593. [CrossRef]

19. Nisar, K.S.; Farman, M.; Abdel-Aty, M.; Ravichandran, C. A review of fractional order epidemic models for life sciences problems: Past. *Alex. Eng. J.* **2024**, *95*, 283–305. [CrossRef]
20. Riaz, M.; Khan, Z.A.; Ahmad, S.; Ateya, A.A. Fractional-Order Dynamics in Epidemic Disease Modeling with Advanced Perspectives of Fractional Calculus. *Fractal Fract.* **2024**, *8*, 291. [CrossRef]
21. Sintunavarat, W.; Turab, A. Mathematical analysis of an extended SEIR model of COVID-19 using the ABC-fractional operator. *Math. Comput. Simul.* **2022**, *198*, 65–84. [CrossRef]
22. Panwar, V.S.; Uduman, P.S.; Gómez-Aguilar, J. Mathematical modeling of coronavirus disease COVID-19 dynamics using CF and ABC non-singular fractional derivatives. *Chaos Solitons Fractals* **2021**, *145*, 110757. [CrossRef]
23. Lamwong, J.; Pongsumpun, P. Modeling the spread of hand, foot, and mouth disease using ABC fractional derivatives: A focus on environmental and vaccination impacts in children. *Model. Earth Syst. Environ.* **2025**, *11*, 118. [CrossRef]
24. Zadeh, L.A. Fuzzy sets. *Inf. Control* **1965**, *8*, 338–353. [CrossRef]
25. Subramanian, S.; Kumaran, A.; Ravichandran, S.; Venugopal, P.; Dhahri, S.; Ramasamy, K. Fuzzy fractional Caputo derivative of susceptible-infectious-removed epidemic model for childhood diseases. *Mathematics* **2024**, *12*, 466. [CrossRef]
26. Qayyum, M.; Fatima, Q.; Akgül, A.; Hassani, M.K. Modeling and analysis of dengue transmission in fuzzy-fractional framework: A hybrid residual power series approach. *Sci. Rep.* **2024**, *14*, 30706. [CrossRef]
27. Muhammad, G.; Akram, M. Fuzzy fractional epidemiological model for Middle East respiratory syndrome coronavirus on complex heterogeneous network using Caputo derivative. *Inf. Sci.* **2024**, *659*, 120046. [CrossRef]
28. Aldwoah, K.A.; Almalahi, M.A.; Hleili, M.; Alqarni, F.A.; Aly, E.S.; Shah, K. Analytical study of a modified-ABC fractional order breast cancer model. *J. Appl. Math. Comput.* **2024**, *70*, 3685–3716. [CrossRef]
29. Khan, H.; Alzabut, J.; Gómez-Aguilar, J.; Alkhazan, A. Essential criteria for existence of solution of a modified-ABC fractional order smoking model. *Ain Shams Eng. J.* **2024**, *15*, 102646. [CrossRef]
30. Almalahi, M.A.; Aldwoah, K.A.; Shah, K.; Abdeljawad, T. Stability and numerical analysis of a coupled system of piecewise atangana–baleanu fractional differential equations with delays. *Qual. Theory Dyn. Syst.* **2024**, *23*, 105. [CrossRef]
31. Bede, B.; Stefanini, L. Generalized differentiability of fuzzy-valued functions. *Fuzzy Sets Syst.* **2013**, *230*, 119–141. [CrossRef]
32. Allahviranloo, T.; Salahshour, S.; Abbasbandy, S. Explicit solutions of fractional differential equations with uncertainty. *Soft Comput.* **2012**, *16*, 297–302. [CrossRef]
33. Allahviranloo, T.; Ghanbari, B. On the fuzzy fractional differential equation with interval Atangana–Baleanu fractional derivative approach. *Chaos Solitons Fractals* **2020**, *130*, 109397. [CrossRef]
34. Atangana, A.; Baleanu, D. New fractional derivatives with nonlocal and non-singular kernel: Theory and application to heat transfer model. *Therm. Sci.* **2016**, *20*, 763–769. [CrossRef]
35. Crowley, P.H.; Martin, E.K. Functional responses and interference within and between year classes of a dragonfly population. *J. N. Am. Benthol. Soc.* **1989**, *8*, 211–221. [CrossRef]